Investigating Indian summer monsoon in coupled regional land–atmosphere downscaling experiments using RegCM4

D. Kumar[1] · P. Rai[1] · A. P. Dimri[1]

Abstract

The ability of Regional Climate Model (RCM: RegCM4) forced with two different Global Climate Model (GCM: CCSM4 and MIROC5) and three land-surface parameterization (LSP) (i.e., BATS, CLM4.5 and Subgrid-BATS) in simulating the Indian summer monsoon (ISM) is tested for the present climate (1975–2005). Thus six simulation combinations are assessed for seasonal mean temperature, precipitation, and low-level wind for ISM season (June, July, August, September: JJAS) over the COordinated Regional climate Downscaling EXperiment-South Asia (CORDEX-SA) domain. The simulations are evaluated in terms of Taylor's metric (for precipitation, temperature, zonal wind, meridional wind and total cloud fraction), mean annual cycle, index of agreement, normalized root mean squared deviation and probability distribution function. The experiments simulated moderate events more accurately than high-intensity precipitation events compared to the corresponding observations. The inherent biases in the model simulations are attributed to the weaker meridional wind along with restrained vertical motion during ISM, especially with CCSM4 forcing. A careful analysis of tropospheric temperature gradient (TTG) suggests a weaker north–south (N–S) gradient due to the warmer atmospheric column in these experiments. On the contrary, the MIROC5_CLM4.5 experiment captures the magnitude and the temporal evolution of TTG better during ISM. It also represents the mean features of ISM better than other experiments. Also, the CLM4.5 LSP shows promising performance in ISM simulation when forced with MIROC5. It also provides further avenues for testing of the same combination under different frameworks, including the intended future climate study. This study emphasizes the importance of using appropriate GCM and LSP forcings to the RCM for simulating a coupled complex systems such as ISM.

Keywords RegCM4 · CLM4.5 · Indian Summer Monsoon · CORDEX-South Asia · Downscaling

1 Introduction

Indian Summer Monsoon (ISM) is an embedded feature of the large-scale global circulation, which not only contributes to the regional scale precipitation but also affects the global climate variability. It brings approximately 75–80% of the total annual rainfall over the Indian landmass during June to September each year (Rajeevan et al. 2013; Dhar and Nandargi 2003). As the most of the Indian economy depends on crop/agriculture, ISM serves as a lifeline for a large population across India and adjacent regions. ISM, a coupled system described as the seasonal reversal of winds, is characterized by the variability at different spatial and temporal scales. The temporal variability includes at daily, monthly, intra-seasonal, inter-annual, decadal and centennial time-scales. Also, there are active and break periods during ISM at the sub-seasonal scale (Goswami and Mohan 2001; Goswami 2005; Maharana and Dimri 2016; Rai et al. 2018). In addition, variability in the onset, duration and progression of ISM exerts strong control over different sectors such as water resources, agriculture, economy, ecosystem and extremes. Apart from distinct characteristic of ISM and its variability, there are various external (large scale) and internal drivers which as well influence its overall dynamics. These factors include the remote climate phenomena such as El Niño Southern Oscillations (ENSO) (Pant and Parthasarathy 1981; Mooley and Parthasarathy 1983; Gadgil

✉ A. P. Dimri
apdimri@hotmail.com

1 School of Environmental Sciences, Jawaharlal Nehru University, New Delhi, India

et al. 2004; Kumar et al. 2006), Eurasian snow cover (Hahn and Shukla 1976; Dash et al. 2005), Atlantic Multi-Decadal Oscillations (Goswami et al. 2006a) and Indian Ocean Warming (Roxy et al. 2015). Many modeling experiments are employed to study the past, present and future of ISM. These included the output of regional and global climate models as well as their ensemble at different time-scales. The internal factors affecting the ISM are land-surface processes (Meehl 1994; Saha et al. 2011), orography/topography, vegetation and landuse/cover (Chakraborty et al. 2002; Fennessy et al. 1994). At times, the understanding of ISM is constrained by limited observations in terms time, their spatial coverage and the availability of different meteorological variables. This may be one of the reasons that no clear long-term trend could be detected in the seasonal rainfall and its inter-annual variability over the Indian landmass (Kripalani et al. 2003; Guhathakurta and Rajeevan 2008). Ambiguous behavior of the ISM is reported which ranges between significantly negative to positive trends, some insignificant trends, over different sub-regions of India (Kumar et al. 1992; Guhathakurta and Rajeevan 2008). Although no significant long-term trends prevail for the ISM rainfall, there has been an increase in the frequency and magnitude of extreme events during the ISM rainfall (Goswami et al. 2006b; Rajeevan et al. 2006). Thus, to investigate the potential impact and the associated changes in the ISM rainfall, it is necessary to explore other possible tools and techniques. This emphasizes the need for dynamical models for studying different underlying processes of ISM for the present, past and future. The simulation and prediction of ISM using dynamical models is a challenging task due to the inherent instability and the multi-scale complex interactions between large-scale circulations and local scale physical processes (Mohan and Goswami 2003). Previously, efforts were made to investigate the representation of mean features of ISM in Global Climate Models as well as Regional Climate Models (hereafter GCMs and RCMs respectively). Bhaskaran et al. (1996) used a nested RCM and shown that it captured the mean and intra-seasonal variability of ISM similar to the GCM forcing. Jacob and Podzun (1997) used a seasonal scale RCM simulation to represent ISM and found that boundary conditions are dominant factors in regional-scale simulation. Ji and Vernekar (1997) also used a nested RCM to simulate contrasting years of ISM and suggested that the phase and amplitude of the mean and variability are realistically simulated. Dash et al. (2006) used the RegCM3 model to show that the mean monsoon simulation is sensitive to the snow depth over Tibet during April. Singh and Oh (2007) explained the sensitivity of ISM to the warmer sea surface temperature (SST) anomaly over the Indian Ocean. Saeed et al. (2009) used the RCM framework to study the importance of representation of irrigation in models to improve the simulation of ISM. The WRF model

was found to reasonably simulate the inter-annual variations of ISM in a high-resolution simulation (Srinivas et al. 2013). Ratnam et al. (2009) used a coupled regional atmosphere–ocean modeling framework to simulate improved ISM mean features and intra-seasonal variability. The intra-seasonal variability of ISM using RCMs has also been investigated in many studies (Bhaskaran et al. 1998; Bhate et al. 2012; Maharana and Dimri 2016; Umakanth et al. 2016). It is evident from previous efforts that RCM simulations are sensitive to different factors namely: the choice of physical parameterizations of convection, clouds, planetary boundary level, land surface etc. Besides, it is affected by choice of domain size, initial and lateral boundary forcing, representation of orography etc. These factors impart a considerable amount of uncertainties to the regional climate simulations and thus it is important to handle the same with the correct approach. Previous RCM studies based on ISM over India have mostly focused on the selection of appropriate parameterization schemes (Alapaty et al. 1994; Dash et al. 2006; Ratnam and Cox 2006; Mukhopadhyay et al. 2010; Singh et al. 2011; Giorgi et al. 2012; Srinivas et al. 2013; Raju et al. 2015; Ali et al. 2015; Bhatla et al. 2016; Nayak et al. 2017; Maity et al. 2017a, b; Sinha et al. 2019). Most of the studies mentioned above have used the reanalysis datasets to force their downscaling experiments, while few of them have downscaled the GCMs. The selection of GCM forcing in most of these experiments did not follow a particular reason for their selection for downscaling. Therefore, in the current study, the GCM selection for downscaling experiments has been made based on available literature as part of an independent exercise (refer Sect. 2.1). The idea behind such selection is to explore the efficacy and efficiency of dynamically downscaled GCM products in simulating the ISM rainfall and associated features. Moreover, most of the previous studies using RegCM chose the default Biosphere–Atmosphere Transfer Scheme (BATS) model for the representation of land-surface hydrology and other processes for ISM simulation. Very less information is available regarding the performance of the CLM4.5 model in coupled RegCM4 framework for monsoon simulation. Therefore, the current study is based on two major objectives

1. Investigation of efficacy and efficiency of the GCM selection on the simulation of ISM.
2. Investigation of the performance of the CLM4.5 land surface model coupled in a RegCM4 framework for simulation of ISM.

Previous studies over the COordinated Regional climate Downscaling EXperiment-South Asia (CORDEX-SA hereafter) region do not provide a clear overview of the overall performance of RCM experiments. Few studies indicate no value addition in RCM simulations for most of the ISM

features, while a few show improvement in representing the spatial distribution and the amount of precipitation (Mishra et al. 2014; Singh et al. 2017; Choudhary et al. 2019). In general, the emphasis has been given over the necessity of a coupled regional land–atmosphere–ocean framework for accurately representing the land–atmosphere–sea interactions during the ISM (Singh et al. 2017). Given this, the current study may provide further avenues for exploring the importance of a coupled land–atmosphere downscaled information for larger coordinated efforts like CORDEX. This study will help in understanding the relative benefit and the shortcomings of the RegCM4 modeling system using the BATS and CLM4.5 land-surface parameterization schemes over the CORDEX-SA. In subsequent sections, details of Data and methodology, Results and discussion, Summary and conclusions are presented.

2 Data and methodology

In the current framework, two different types of the dataset including the observation and the model simulation, are used. The observation datasets are used for the validation of the simulated model experiments. Daily gridded precipitation dataset over Indian landmass from India Meteorological Department at the horizontal resolution of 50 km (Rajeevan and Bhate 2009) is used for rainfall validation. For temperature validation, a monthly temperature climatology dataset from the Climatic Research Unit (Harris and Jones 2017) is utilized. For other basic fields such as U-wind, V-wind, Omega and Specific humidity, the reanalysis dataset from ERA-Interim (Dee et al. 2011) is used.

2.1 Selection of GCM

As it is well known that, the downscaling approach has its dependency over the GCMs for the initial and lateral boundary conditions. In the present framework, the selection of appropriate GCM forcing has been done based on the currently available pieces of literature on ISM. The objective criterion for the selection of models has been considered in terms of the representation of different ISM features for the present climate. These features include seasonal mean ISM rainfall, inter-annual, intra-seasonal variability and mean annual cycle of ISM rainfall. This exercise suggests that no single model is perfect in simulating these features of monsoon in most of the studies. However, two GCMs namely CCSM4 and MIROC5 were found to be the appropriate forcing as suggested in many studies (Menon et al. 2013; Mishra et al. 2014; Babar et al. 2015; Sooraj et al. 2015; Sarthi et al. 2015, 2016; Sharmila et al. 2015; Jena et al. 2016; Prasanna 2016; Meher et al. 2017; Das et al. 2018). The evaluation of the downscaled output becomes even relevant in the sense

that; these models have not been downscaled using any RCM as part of CORDEX programme previously especially over South Asia or Indian Region. The prognostic variables (U, V, Q, PS, and TA), as well as SST for the RCM simulations, were obtained from the Earth System Grid Federation portal for CMIP5 (https://esgf-data.dkrz.de/projects/esgf-dkrz/) for MIROC5 and Climate data gateway of NCAR (https://www.earthsystemgrid.org/) for CCSM4.

2.2 The Regional Climate Model

The Regional Climate Model (RegCMv4.7) developed and managed at the International Centre for Theoretical Physics (ICTP) has been used for the downscaling experiments in this study. It is an evolved version of RegCM3 with improved physical parameterization and other features with enhanced performance over the tropical regions (Giorgi et al. 2012) as compared to previous releases. The model is compressible, hydrostatic and equipped with terrain-following σ-coordinate vertically. In the recent versions of RegCM4, a new feature of a mixed type convection scheme has been added. Giorgi et al. (2012) have shown that such mixed type schemes have capabilities to improve the simulation of climate over different regions across different CORDEX domains in the world. RegCM4 has been used for a range of studies around the globe including seasonal to annual, decadal and climate change simulations. In RegCM4, U and V velocity fields are represented at the dot points while the temperature, pressure and relative humidity values are prescribed at cross points following the Arakawa-B type grid staggering. In addition to the cumulus parameterization in the model, radiative transfer scheme of NCAR model CCSM3 (Kiehl et al. 1996), planetary boundary layer (PBL) parameterization of Holtslag (Holtslag et al. 1990) and University of Washington PBL scheme (Bretherton et al. 2004) have been included in the new versions. Moreover, the parameterization for cloud microphysics, large scale resolvable precipitation using Subgrid explicit Moisture (SUBEX) scheme (Pal et al. 2000), ocean flux parameterization, interactive aerosols and chemistry, and lake models have also been incorporated gradually.

2.3 Land surface models

Besides the regular parameterization of cumulus convection, large-scale precipitation, microphysics, PBL, etc., LSP is one of the important aspects of RCMs. It is vital in the sense that it facilitates the exchange of energy and moisture with the atmosphere through the PBL and hence affect the partitioning of fluxes among different components. In the current versions of RegCM4, three different LSPs namely: Biosphere Atmosphere Transfer Scheme (BATS; Dickinson et al. 1993), Community Land Model 3.5, and the

more recent Community Land Model 4.5 (with an update to CLM3.5) are available for representation of different land-surface processes. Besides, the RegCM framework also facilitates a subgrid disaggregation of the topography and land use features, which is a modification to the existing BATS scheme (Giorgi et al. 2003). While using subgrid disaggregation, a mosaic-type approach is considered to disaggregate the coarser grid into the prescribed number of finer subgrids. Further, the input meteorological variables are disaggregated from the parent grid to the finer subgrids while accounting for the elevation differences among grids. The calculations are performed using BATS at these subgrids individually and the fluxes are re-aggregated to the parent grid after simple averaging. The subgrid technique does not facilitate the disaggregation of precipitation and this approach does not affect precipitation formation directly. However, it is found that ISM rainfall formation mechanisms in the case of the subgrid approach has higher sensitivity due to the dominance of convective precipitation and dominant feedback of surface fluxes. A detailed account of the differences in the formulations of these land surface models can be found in section 2.1.1 in Kumar and Dimri (2019).

2.4 Experimental design

For the simulation of ISM during the present climate, six different long term simulations for the present climate (1970–2005) were carried out using the combination of two different GCMs (Sect. 2.1) and three different land-surface experiments. The model integrations were carried

out from 1st January 1970 up to 31st December 2005 for each set of experiments with 5 years of spin-up period. The domain used for the simulation extends 10–130° E and 20°S–50° N and known as CORDEX-SA domain (Fig. 1). The domain is adequately large to develop its large-scale monsoonal circulation and the cross-equatorial flow. The horizontal and vertical resolution of the 6-hourly initial input data is available at $0.9424° \times 1.25° \times 26$ (lat, lon, z) and $1.4008° \times 1.40625° \times 40$ (lat, lon, z) for CCSM4 and MIROC5 respectively. While the SST at the lateral boundary is monthly time series at a spatial resolution of 1° similar to initial data (lat, lon) for CCSM4 and MIROC5 GCMs were used. The CCSM4 input data belongs to r6i1p1 ensemble experiments while for the MIROC5 input data, it is obtained from r1i1p1 ensemble experiments. In addition to the initial and boundary data, the static datasets were obtained from different sources. The input of topography has been obtained from the GMTED dataset of the United States Geological Survey (USGS) while the land cover data has been obtained from Global Land Cover Characterization for BATS (hereafter Control) and subgrid disaggregation of BATS (hereafter SUB-BATS) experiments. In the case of CLM4.5, the plant functional types were prescribed from National Centre from Atmospheric Research (NCAR) datasets. For the CLM4.5 set of experiments, MIT-Emanuel convection scheme over land and ocean has been used. On the other hand, Grell over land and ocean were used for BATS and SUB-BATS experiments. The detailed model configuration is presented in Table 1. The acronyms for different experiments, their

Fig. 1 Surface elevation (m) over the study area (20° S–50° N and 10–130° E, CORDEX-South Asia domain)
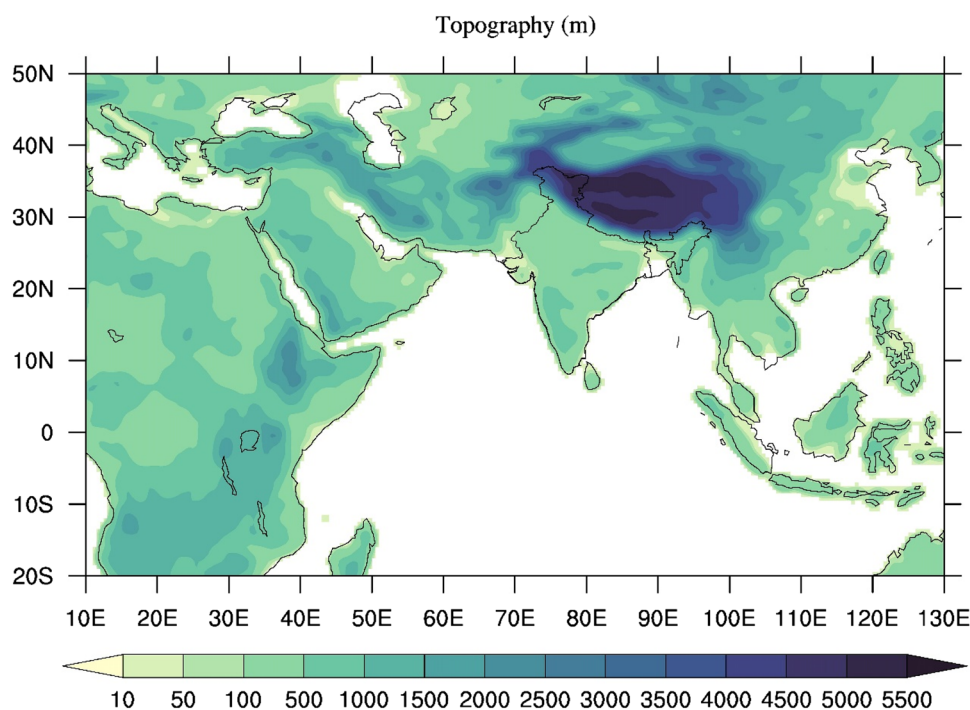

Topography (m)

Table 1 Model configuration used in the study

Dynamics	Hydrostatics
Regional Climate Model	RegCM4.7
Model domain	CORDEX-South Asia (10–130° E and − 22° S–50° N)
Resolution	50 km (~0.44°) horizontal and 18 σ-levels
GCM forcing	MIROC5 and CCSM4 (u, v, t, q, ps and SST)
Radiation parameterization	Modified CCSM3
Planetary boundary layer	Modified Holtslag
Period	1970–2005, 5 years as spin up

corresponding LSPs, and cumulus parameterizations have been described in Table 2.

2.5 Methodology

In the current study, the initial 5 years of simulation have been discarded to allow the land-surface model to attain the dynamic equilibrium in the land surface hydrology. In general, the spin-up period for regional climate simulation varies from 10 days to 1 month depending upon the application (Wang et al. 2003; Rao et al. 2004; Ratnam and Kumar 2005; Martínez-Castro et al. 2006; Kang et al. 2014). In many experiments, while using CLM as a land surface model for regional simulations, 1 month of spin-up time was found to be sufficient (Maity et al. 2017b; Tiwari et al. 2015, 2017; Gao et al. 2016; Maurya et al. 2018). It was shown that over dry land areas, the spin-up of land surface state takes approximately 2–3 years while over monsoon regions such stabilization is achieved in about 3 months if the integration is started just before the onset of monsoon (Lim et al. 2012). Based on the above literature, it is believed that 5 years of spin-up period is sufficient for climatological scale simulations to achieve the dynamical equilibrium of the internal physics of the model. From the simulated output for the period (1975–2005), the June–September (JJAS) daily mean climatology of near-surface air temperature, mean low-level jet at 850 hPa and daily mean ISM rainfall have been calculated and compared with the corresponding observations.

Moreover, for the assessment of model performance in simulating ISM, the mean bias in temperature and precipitation fields have been computed. For the evaluation of inter-annual variability in the model experiments, the mean annual cycle, the standard deviation of precipitation has also been computed. Moreover, for highlighting the weakness of the model experiments in simulating different precipitation intensities with the season, probability distribution function (PDF) has been calculated. Further, different statistical metrics to facilitate the comparison of model performance have been calculated as discussed below:

1. Normalized root mean squared error (NRMSE)

The root mean squared error (RMSE) is quite useful in summarizing the mean difference between the simulated and observed values and described as

$$RMSE = \sqrt{\frac{\sum_{i=1}^{n}(O_{mi} - S_{mi})^2}{n}} \tag{1}$$

In Eq. (1), O_{mi} and S_{mi} correspond to observed and simulated values for the particular year i. For precipitation, normalized RMSE to describe the mean deviation of each experiment with respect to observations has been calculated as

$$NRMSE = \frac{RMSE}{\bar{O}} \tag{2}$$

2. Willmott's index of agreement (IOA)

To facilitate a comparison between model simulation and the observation, an index was developed by Willmott (1982). It is defined as

Table 2 Combination of land surface and cumulus parameterization used in different experiments

Land surface model (cumulus parameterization) →	Control (BATS) (Grell over land and ocean)	SUB-BATS (Grell over land and ocean)	CLM4.5 (MIT-Emanuel over land and ocean)
GCM ↓			
CCSM4	CCSM4_Control	CCSM4_SUB-BATS	CCSM4_CLM4.5
MIROC5	MIROC5_Control	MIROC5_SUB-BATS	MIROC5_CLM4.5

$$d = 1 - \frac{\sum (F_i - O_i)^2}{\sum \left(|F_i - \bar{O}| + |O_i - \bar{O}| \right)^2}. \qquad (3)$$

Here, F_i and O_i are the forecast and observation for ith year, while. '$\bar{O}$' represents their climatology for the period under study. IOA has the acceptable range as 0–1, where 1 corresponds to the perfect score for this index meaning the best performance.

3. Taylor's diagram

Taylor's diagram (Taylor 2001) facilitates quantification of how closely two patterns match with each other. It is quantified in terms of their pattern correlation; centered root mean squared difference and the standard deviation. These diagrams are quite useful in comparison of the performance of multiple models. The models having the highest correlation coefficient, standard deviation similar to observation, and minimum root mean squared deviation is usually considered as the best performing model. Taylor's metrics have been computed from the area average over the Indian landmass region.

Also, to further investigate the dynamics associated with each model experiment leading to their peculiar behavior in ISM simulation, different quantities such as Vertically Integrated Moisture Flux Convergence and its transport (VIMT) and Latitude–Pressure cross-section of Omega has also been used. The moisture flux convergence integrated over 1000–300 hPa has been computed following Fasullo and Webster (2003), Van Zomeren and Van Delden (2007) as

$$VIMFC = -\frac{1}{g} \int_{1000\,hpa}^{300\,hpa} \left(\frac{\partial uq}{\partial x} + \frac{\partial vq}{\partial x} \right) dp \qquad (4)$$

where q is specific humidity, u and v are zonal and meridional components of wind, p represents the pressure and g is the acceleration due to gravity. The assessment of the simulation of land surface processes in each experiment has been carried out with an inter-comparison of surface fluxes. To investigate the intensity of the simulated monsoon circulation as well as the land–sea gradient, the Tropospheric Temperature Gradient (TTG) has been analyzed. The evolution of the TTG between the northern (15–35° N, 40–100° E) and southern box (15° S–5° N, 40–100° E) during JJAS has been calculated following Xavier et al. (2007).

3 Results and discussion

The results from the stated experiments in the light of different analyses are being discussed in the following paragraphs.

3.1 Near surface air temperature (T_{mean})

The JJAS mean near-surface air temperature (°C) climatology for each individual experiment as well as the Climatic Research Unit (CRU) observation, has been presented in Fig. 2. All the experiments are able to capture the spatial patterns of T_{mean} climatology over the study area. Temperature minima over the Himalayan and the Tibetan plateau region and the maxima over the central and northwestern Indian region are well reproduced in all the experiments. However, the magnitudes of simulated T_{mean} vary considerably among the experiments indicating the differences among experiments. The T_{mean} simulation seems to be affected by the choice of land surface model, as the experiments using CLM4.5 are comparatively warmer than the Control and SUB-BATS experiments. The experiments forced with CCSM4 simulate warmer T_{mean} over the central and northwest Indian region as compared to those forced with MIROC5. Important to mention is that similar warmer climatology over the Indian region in a land–atmosphere model was reported by Raju et al. (2015). Moreover, colder T_{mean} climatology over the higher reaches of western Himalaya has been simulated in CLM4.5 experiments as compared to Control and SUB-BATS experiments. The Control and SUB-BATS experiments forced by CCSM4 and MIROC5 also have considerable differences in the magnitude of simulated T_{mean}. This manifests as the warmer (colder) T_{mean} over the Indian landmass in the case of CCSM4 (MIROC5) GCM experiments. The Control and SUB-BATS experiments portray similar T_{mean} climatology for the same forcing case. For example, the CCSM4_Control and CCSM4_SUB experiments show similar JJAS mean climatology for T_{mean} over most part of the Indian landmass irrespective of their different LSP. This also applies to the Control and SUB-BATS experiments forced with the MIROC5 GCM. It is again noteworthy that, Control and SUB-BATS experiments have the same cumulus parameterization scheme for the simulation period. The inter-model differences in the simulation of T_{mean} may thus also be related to the differences in the cumulus parameterization for different experiments. In general, the experiments namely CCSM4_Control and CCSM4_SUB, seem to simulate greater resemblance in the spatial features of T_{mean} as compared to the observation. Further, MIROC5_Control and MIROC5_SUB experiments have comparatively colder T_{mean} climatology than observations over the higher reaches of the Himalayas and the Tibetan highlands. To further investigate the spatial patterns of discrepancies in the model simulated T_{mean}, their mean bias has been presented in Fig. 3. The daily T_{mean} bias for JJAS season suggests that all the experiments have a considerable magnitude of biases along with consistent inter-model differences in their spatial distribution. Conforming
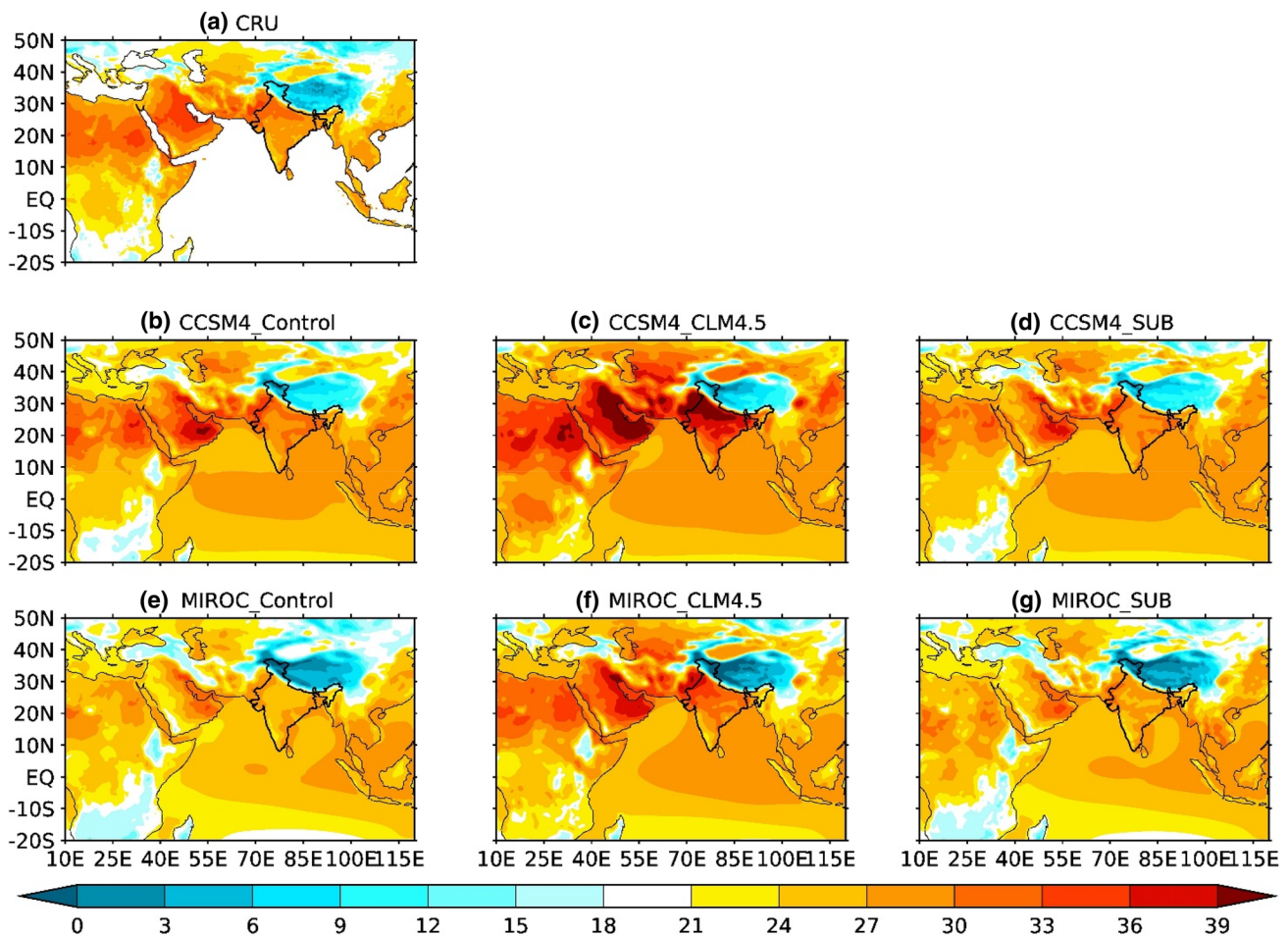
Fig. 2 JJAS mean near surface air temperature climatology (°C) for the period 1975–2005 for CRU observation (**a**) and different model experiments (**b–g**) over the study area

to the warmer climatology in CCSM4 forced experiments, slight warm bias has been noted in these sets of experiments. Positive T_{mean} biases over northwest India have also been reported in previous studies (Lucas-Picher et al. 2011; Saeed et al. 2009). Saeed et al. (2009) attributed such overestimation to occur because, in general, the irrigation patterns over Pakistan are not well represented in model simulations. This also concludes that the LSPs seem to affect the T_{mean} simulation possibly due to their different formulation in the calculation of surface fluxes. Interestingly, the bias patterns in the case of Control and SUB-BATS experiments are opposite to each other for CCSM4 and MIROC forced experiments. This indicates the importance of GCM forcing in an accurate simulation of T_{mean}. Although the CLM4.5 experiments with both the forcing simulates warm biases over most parts of Indian landmass, its magnitude is again less with MIROC5 as forcing GCM. Overall, for the simulation of T_{mean}, the CCSM4_Control and CCSM4_SUB experiments seem to outperform other experiments due to a comparatively lesser magnitude of

biases in them. In Fig. 3d, the MIROC5_Control experiment shows a slight to moderate cold bias over the central, peninsular and northern part of India. Such biases are reduced while using SUB-BATS (Fig. 3e) land surface model. Similarly, the slight warm bias in CCSM4 Control experiments is also improved by their SUB-BATS counterpart (Fig. 3a, c). The improvement in T_{mean} simulation is contrary to that reported by Dimri and Niyogi (2013) for the western Himalayas during winter season, where SUB-BATS experiments exhibited colder climatology by a magnitude of 2–4 °C. Furthermore, as reported by Giorgi et al. (2003), SUB-BATS experiments show promising performance in improving the T_{mean} simulation over a complex terrain like western, central and eastern Himalayan regions. The warmer T_{mean} climatology over northwest India has also been revealed in previous studies (Saeed et al. 2009; Lucas-Picher et al. 2011). Saeed et al. (2009) have further explained such underestimation to occur because of the missing representation of irrigation over regions of Pakistan is regional climate simulations.
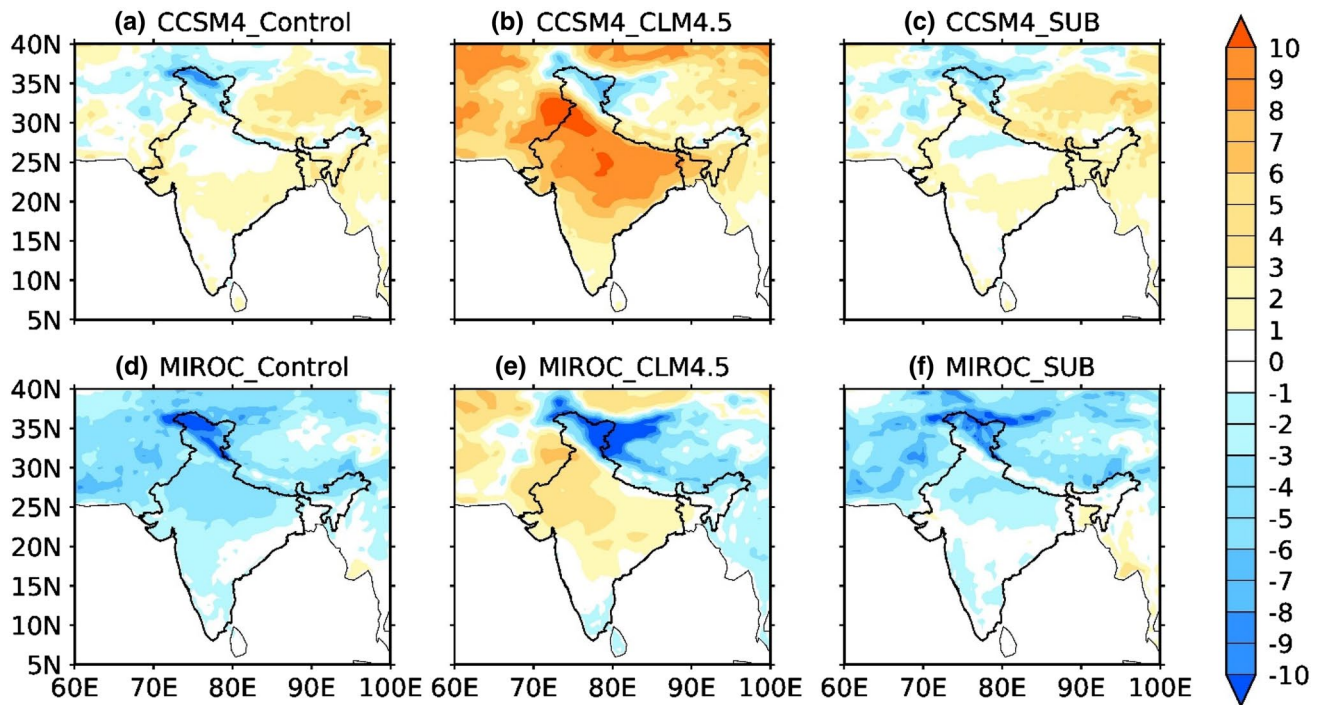
Fig. 3 Bias of JJAS mean near-surface air temperature climatology (°C) for the period 1975–2005 against CRU observation (**a**) and different model experiments (**b**–**g**) over the study area

3.2 Vertically integrated moisture flux convergence and the mean circulation

Further, we investigate the efficiency of model experiments in simulating the mean monsoonal circulation and the over-all moisture transport towards the Indian landmass region. For this sake, the VIMFC, along with its transport by monsoonal winds at 850 hPa, is presented in Fig. 4. The VIMFC is calculated by vertically integrating the horizontal moisture flux convergence/divergence between the surface and 300 hPa vertical levels (Eq. 4). Following the sign convention, negative (positive) values of VIMFC represents convergence (divergence) in Fig. 4. During the JJAS season, the spatial patterns of VIMFC suggest a convergence along the coast of Somalia and the northern Arabian Sea, which is further transported towards the Indian landmass by the cross-equatorial flow at 850 hPa thus leading to the moisture incursion from the ocean towards the land (Fig. 4a). Evidently, the southern Indian Ocean and the Arabian Sea serve as a significant source of moisture for the Indian region during monsoon months. Further, the major convergence zones over the Indian landmass lies along the Western Ghats, northern India, Indo-Gangetic plains, and parts of northeast India. For the northeast Indian region, the moisture transport originates in the Bay of Bengal (BoB). The transport of the converging moisture from the southern BoB and Western Ghats region sets up conducive conditions for the monsoonal precipitation over other parts of the Indian landmass. While discussing the performance of individual model experiments in simulating the mean circulation features, it is found that the Control and SUB-BATS simulations have weaker cross-equatorial flow and moisture convergence as compared to the ERA-Interim reanalysis (Fig. 4b, d and e, g). Such a feature is prominently seen across all the Control and SUB-BATS simulations despite their different GCM forcing. For these simulations, weaker moisture convergence off the coast of Somalia and the northern Indian Ocean is noticed. This in association with weaker south-westerlies is incapable of transporting the moisture towards landmass and therefore have implications for the rainfall distribution in case of these experiments. Among all the experiments, the MIROC5_SUB experiment has the weakest moisture transport with poorly simulated spatial patterns of south-westerlies. Besides, the CCSM4_SUB experiment simulates similar patterns to the former. All the model experiments simulate a higher order of divergence over the Tibetan highlands with even stronger divergence in the case of CCSM4 set of simulations. Unlike Control and SUB-BATS experiments, there is an improvement in the simulation of large-scale circulation and moisture transport while using CLM4.5 as a land surface model in case of both the GCM forcing. In particular, the MIROC5_CLM4.5 experiment portrays a more considerable resemblance to the ERA-Interim reanalysis in the representation of spatial patterns of VIMFC and its transport. The CCSM4_CLM4.5
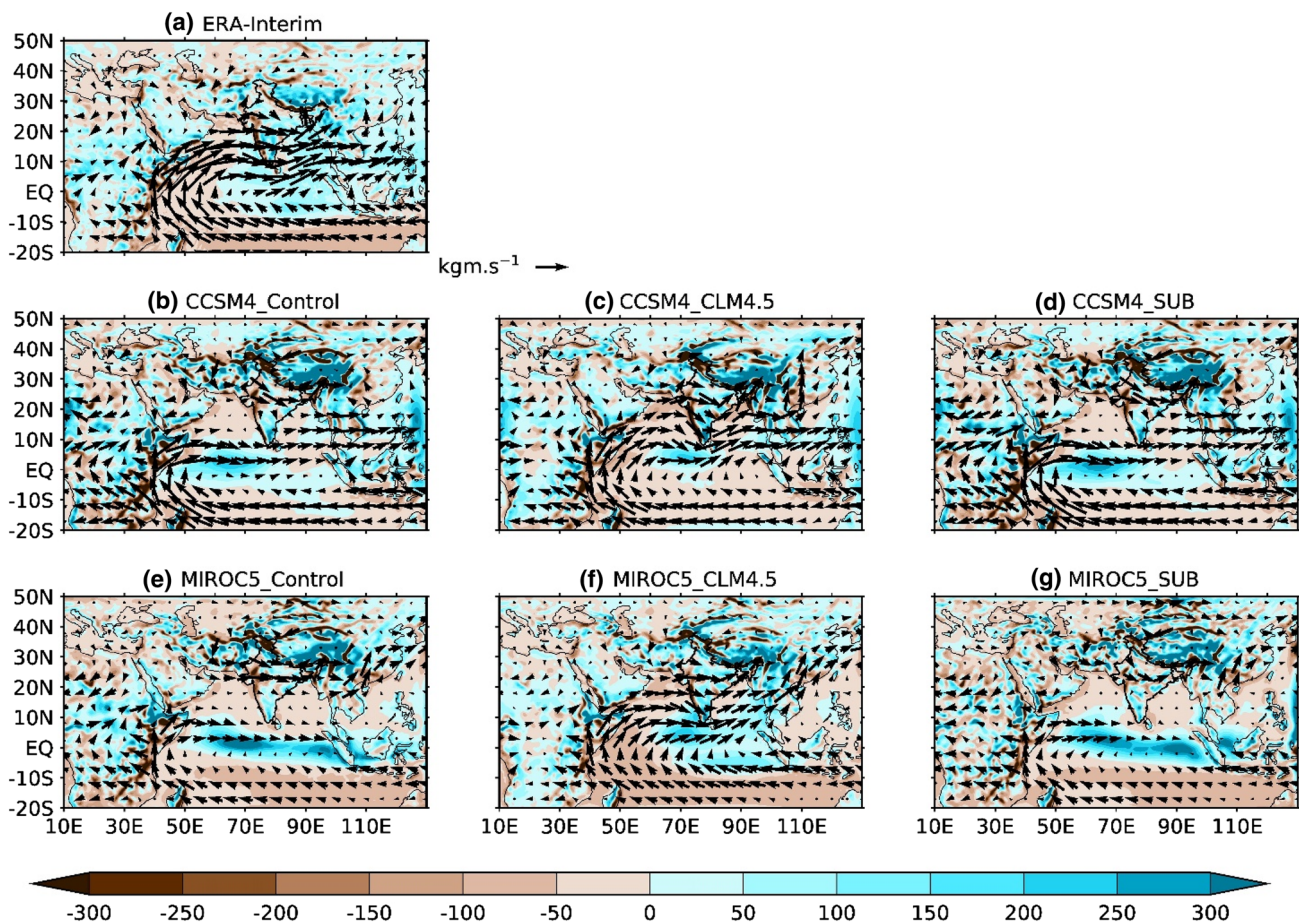
Fig. 4 Vertically integrated moisture flux convergence (shaded) and its transport (vector at 850 hPa) for the JJAS season during 1975–2005 over the study area for ERA-Interim reanalysis (**a**) and different model experiments (**b–g**)

also displays comparable patterns of VIMFC and the mean monsoonal circulation but it has stronger convergence in the southern Indian Ocean and northern BoB. The weaker circulation in the model experiments may be related to the erroneous simulation of mean sea level pressure (MSLP). Experiments with weaker moisture convergence and transport have weaker land–sea gradient as seen from the bias in MSLP over the Indian region. Such experiments have higher MSLP over the land areas thus leading to a significant offset in the intensity and location of southwesterly winds (see supplementary information, Fig. S1). For instance, MIROC5_Control and MIROC5_SUB have positive MSLP bias over Indian landmass unlike CLM4.5 experiments; therefore, possibly a weaker land–sea gradient is associated with them. This feedback can also be noticed in the mean wind circulation at 850 hPa (Fig. S2). The location and magnitude of southwesterly circulation are better captured in case of experiments having lesser MSLP biases over the land. This explains the role of the land–sea pressure gradient in the simulation of appropriate low-level circulation. In the case of the upper-level circulation features, the spatial patterns

of anti-cyclonic flow (at 200 hPa) over central and southern Indian landmass, Tibetan Plateau, equatorial and southern Indian Ocean, mid-latitude regions are well captured in case of CLM4.5 experiments. Further, the location, as well as the magnitude of the tropical easterly jet and the subtropical westerly jet are well-reproduced in CLM4.5 experiments (Fig. S3). Overall, the MIROC5_CLM4.5 experiment could reproduce the mean characteristics of low-level and upper-level circulation features better than other experiments.

3.3 Climatology of ISM rainfall

Figure 5 represents the spatial distribution of the climatological mean of JJAS precipitation from the observation as well as different model experiments. It is evident from both the observation (Fig. 5a, b) that precipitation maxima over the Western Ghats, northeast India, and central Indian region occurs during the monsoon season over Indian landmass. The precipitation from the Global Precipitation Climatology Project (GPCP) dataset has also been presented (Fig. 5b) in order to facilitate the comparison of simulated results over the ocean. It has been
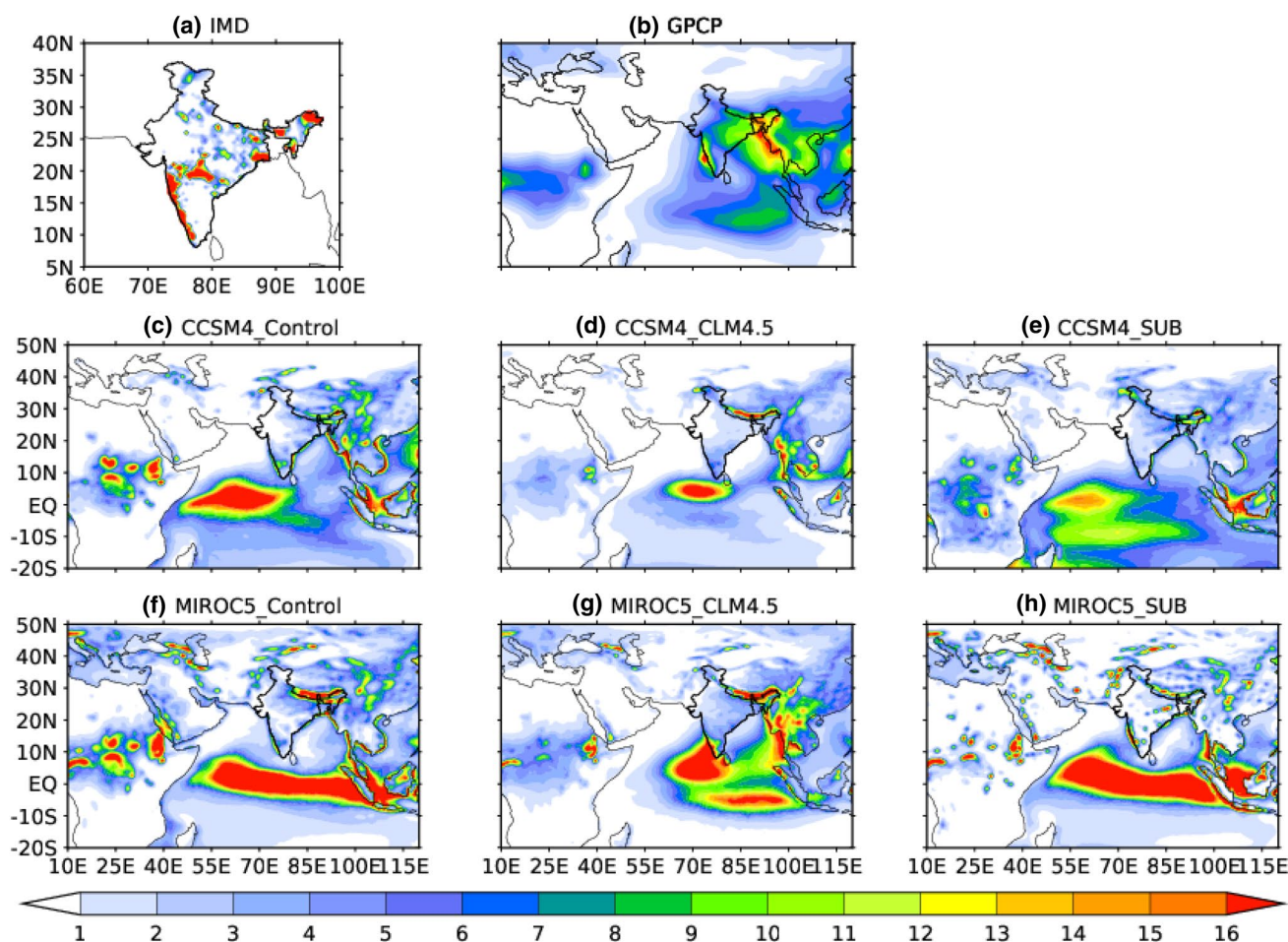
Fig. 5 JJAS daily mean precipitation (mm/day) from **a** IMD over Indian landmass, **b** GPCP observation and different model experiments (**c**–**h**) over the study area for the period 1975–2005

found that the model experiments are able to capture the precipitation patterns over the Indian landmass, but their magnitudes vary significantly. All the experiments seem to underestimate the daily mean precipitation climatology over the Indian region and many of them even do not represent the spatial maxima over the Western Ghats and the central Indian region. The magnitude of precipitation over the Western Ghats in the CCSM4 set of experiments is comparatively less than those forced with MIROC5. Besides, all the experiments seem to have greater precipitation over the ocean as compared to land. Among all the experiments, the MIROC5 set of experiments has a higher magnitude of precipitation over the ocean as compared to its CCSM4 counterpart. This may be related to the incorrect patterns and location of simulated south-westerlies especially for MIROC5_Control and MIROC5_SUB experiments. As south-westerly winds do not traverse towards the Indian landmass in these experiments possibly due to weaker land–sea pressure gradient, they have a band of precipitation maxima over the equatorial Indian ocean. Contrary to this, the MIROC5_CLM4.5 experiment somehow captures the spatial

maxima zones of precipitation better than others do. This may be related to the higher moisture convergence over these precipitation maxima zones. When compared to the GPCP observation, this experiment indicates better resemblance than others. Further, to quantify the errors in the precipitation simulation, the mean bias in precipitation climatology computed against IMD observation has been presented in Fig. 6. The spatial distribution of bias suggests that all the model experiments have considerable biases in the simulation of daily mean precipitation. Most of the models simulate dry bias over the major parts of Indian landmasses such as the Western Ghats, central India and northeast India. On average, the magnitude of such dry biases ranges between 4–6 mm/day for most of the regions. However, the peninsular Indian region and the southern tip of India have a very little magnitude of bias in most of the experiments. This may be related to the fact that these regions are located at the leeward side of Western Ghats and receive less precipitation during monsoon season. Overestimation (underestimation) of precipitation magnitudes over peninsular (central) India was also reported in previous studies (Maurya
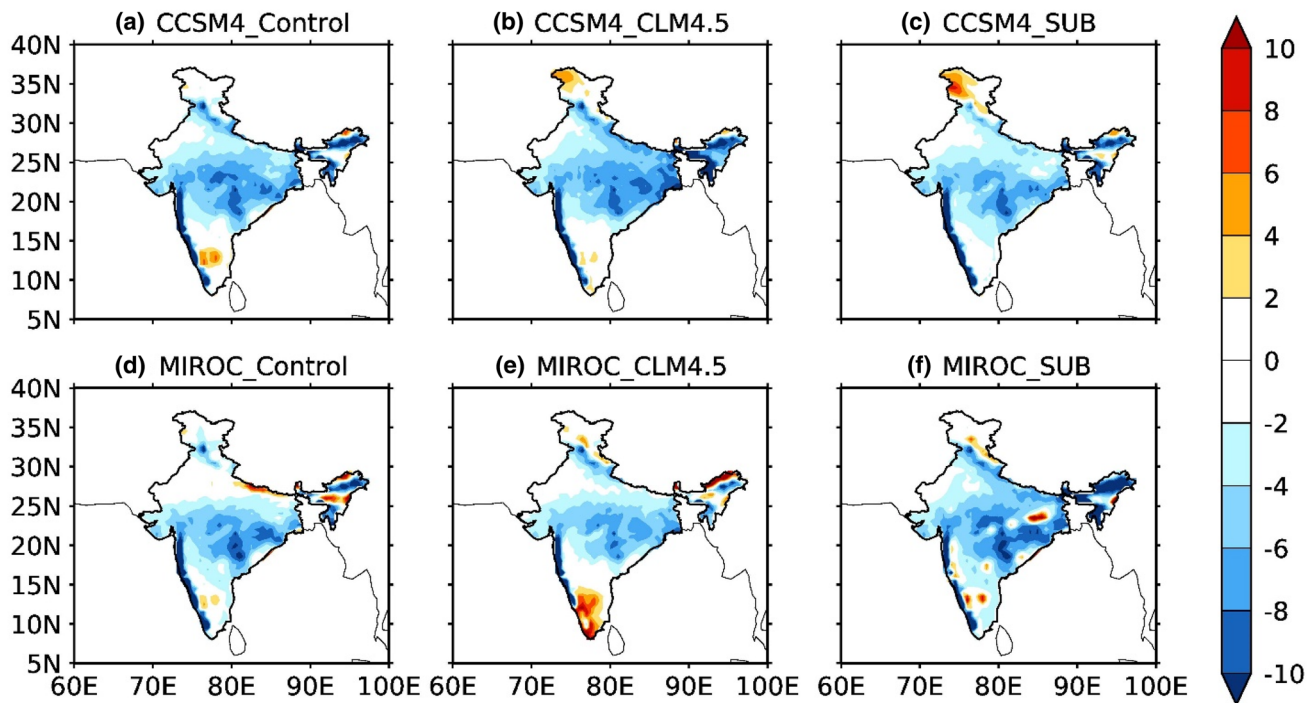
Fig. 6 JJAS mean bias of daily mean precipitation (mm/day) computed against IMD observation from different model experiments

et al. 2017; Nayak et al. 2017; Choudhary et al. 2018). Further, it was reported that the skill of RCM simulation in representing the mean rainfall over central India is constrained by their inability to represent the monsoon depressions. These systems originating in northern BoB plays an important role in bringing precipitation over the central Indian regions. Interestingly, Nayak et al. (2017) suggested the dominance of land surface processes in determining the fate of precipitation over the central Indian region. According to their study, higher Bowen's ratio over central India is simulated in CLM3.5 and BATS experiments. Such interactions result in less surface evaporation thereby limiting the moisture supply to the atmosphere. Dobler and Ahrens (2010) also discussed the underestimation of mean precipitation using the COSMO-CLM model and attributed the same to the weaker representation of dynamics, which results in weaker Monsoon Hadley circulation. They also pointed out the implications of the atmosphere–ocean interaction for good model performance over the ISM region. Another source of error in the RCM simulation is known to propagate from the driving dataset, which further amplifies in the course of downscaling (Iqbal et al. 2017). In addition, the role of cumulus parameterizations has also been underlined in many studies. Previously, it was reported that the MIT-Emanuel scheme produces greater precipitation owing to its feature of auto-conversion of cloud water as precipitation (Giorgi et al. 2012). This trait does not hold for experiments using the Grell scheme, as it does not support the direct mixing of the clouds with the surrounding air. Due to this, the low-level circulation

in Control and SUB-BATS experiments traverses across the southern tip of India instead of rushing towards the central and northern Indian regions. Also, the northern and western Himalayan regions were also found to have lesser biases, and the model experiments overestimate precipitation over these areas. Sinha et al. (2014) using a downscaling experiment, attributed such anomalous and overestimated precipitation to occur due to the topographical uplift in the leeward side of Western Ghats. Furthermore, only two experiments out of total 6 are comparable to each other in terms of mean precipitation bias with somehow similar spatial patterns as well as the magnitude. Again, the MIROC5_CLM4.5 experiment tends to outperform all the other experiments with comparatively less (dry and wet both) biases. This experiment has a lesser magnitude of dry (wet) biases over the central Indian region, northeast India, northwestern Himalaya and the Western Ghats as seen in Fig. 6e. However, wet bias over peninsular India is the highest in this model.

3.4 Spatio-temporal variability of ISM

3.4.1 Mean annual cycle

The mean annual cycle of precipitation computed over the Indian landmass has been presented in Fig. 7. It is a useful metric for comparing the seasonal evolution of precipitation in different model experiments. The annual cycle of precipitation from observation (IMD: black line)

suggests that, with the onset of monsoon in June, the daily mean precipitation increases continuously till July, which represents the peak precipitation intensity (8–9 mm/day). Following this, there is a decline in precipitation intensity for the rest of the months gradually. While comparing model experiments with the observation, strong signatures of dry biases are again visible in the monthly and seasonal evolution of precipitation climatology. This manifests as an incorrect representation of the peak month of precipitation as May instead of July with incomparable magnitudes (ranging between 2–5 mm/day). Interestingly, there is a bi-modal distribution of precipitation with the first peak in May and second in September following an unrealistic dry period during July and August. In terms of the magnitude and seasonal evolution, the MIROC5_CLM4.5 experiment has been found lying close to the IMD observation. Previous studies by Bhatla et al. (2016) have found that the

RegCM model captures the ISM onset very well. However, it has a tendency to simulating excess precipitation during the pre-onset period. This may be one of the reasons for excess precipitation in the months of May–June.

3.4.2 Probability density function (PDF)

For studying the differences in the range of observed and simulated precipitation values, the probability density function is presented in 8. The relative frequency of each precipitation intensity (mm/day) for the JJAS season, averaged over the study area has been calculated. In the case of PDF of precipitation, it reveals the relative frequency of occurrence of rain events of different magnitude. The long tail of the PDF curve here represents the number of similar or high-intensity precipitation events over the period under study. In Fig. 8, the solid black line represents the PDF for observation while others represent different model experiments. Following the strong dry biases in the model experiments, most of them have a high frequency of low to moderate rain events as compared to observation. The PDF of the observation suggests that the rainfall events of 6–7 mm/day have the highest frequency while for most of the experiments, 3–4 mm/day events dominate. Many of the model experiments have very few high-intensity rainfall events across the period of simulation as seen from the width of their distribution curve. Again, the experiments namely: MIROC5_CLM4.5 and CCSM4-SUB stand out in representing the precipitation intensity during the said period. The Control experiments forced with both the GCMs are quite unable to capture the precipitation distribution as compared to the observation and thus due to relative abundance of small precipitation events, they lead to stronger precipitation biases as discussed in previous sections.
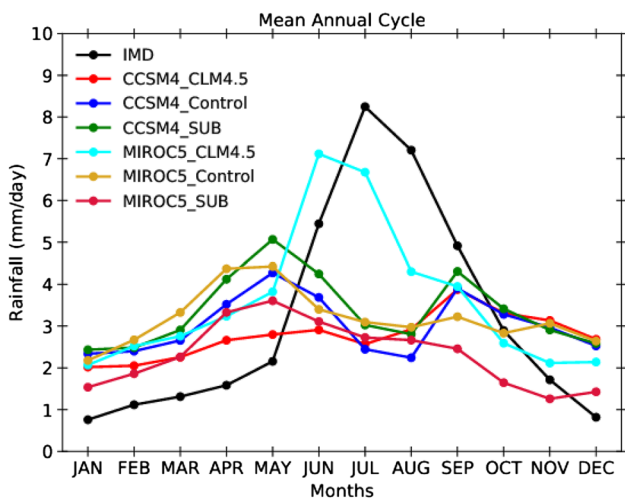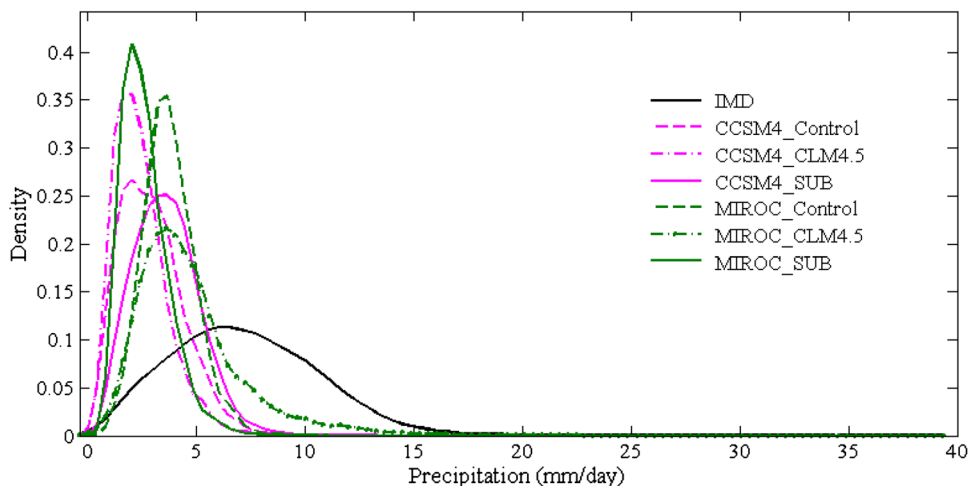

Fig. 7 Mean annual cycle of precipitation averaged over the Indian landmass area from IMD observation (in black) and other experiments for the period 1975–2005

Fig. 8 Probability density functions of daily precipitation from IMD observation (solid black line) and different model experiments

3.5 Statistical validation

In addition to the comparison of the climatology and mean bias, different other statistical metrics have been calculated to gain better insights regarding the performance of the model experiments with special reference to ISM rainfall. The corresponding results to these validation strategies are being discussed here:

3.5.1 Normalized root mean squared error

NRMSE is a commonly used metric for the estimation of differences between the predicted values of a variable from the observed. RMSE has been computed using the mean deviation following the formula given in Eq. (1) and normalized using the observation as per Eq. (2). The value of NRMSE ranges between 0 to 1, with the lower values indicating the perfect forecast. The spatial distribution of NRMSE over Indian landmass has been presented in Fig. 9. It is found that different model experiments exhibit a mixed pattern of model performance in space (in terms of NRMSE). Among the experiments forced with the CCSM4 model, only CCSM4_SUB experiment perform satisfactorily with NRMSE values ranging between 0.5–0.7 over the northern plains, Indo-Gangetic region, and north-east Indian

region. While, peninsular India, north-western Himalaya, Western Ghats and western Indian region seem to be devoid of precipitation and thus higher NRMSE values are portrayed for them. On the other hand, the experiments driven by MIROC5 portray similar spatial patterns of NRMSE. However, there are considerable differences in their magnitude. Among these set of experiments, MIROC5_CLM4.5 display comparatively better performance (lower NRMSE) over northeast India, Indo-Gangetic plains, eastern coast and parts of Western Ghats. Due to the overestimation of precipitation over the southern peninsular region, the calculated NRMSE in the case of this experiment is as high as 1.5 and thus indicates erroneous simulation of precipitation. This feature is consistent in other experiments as well, however, with them, the order of NRMSE is comparatively less.

3.5.2 Index of agreement (IOA)

For studying the similarity between the simulated and observed values, a dimensionless index called Willmott's Index of Agreement (Willmott 1982) have been calculated and presented in Fig. 10. The value of IOA ranges between 0 and 1 for the worse and best forecast, respectively. Coherent to the underestimation of precipitation over major parts of India, most of the experiments reveal lower values of
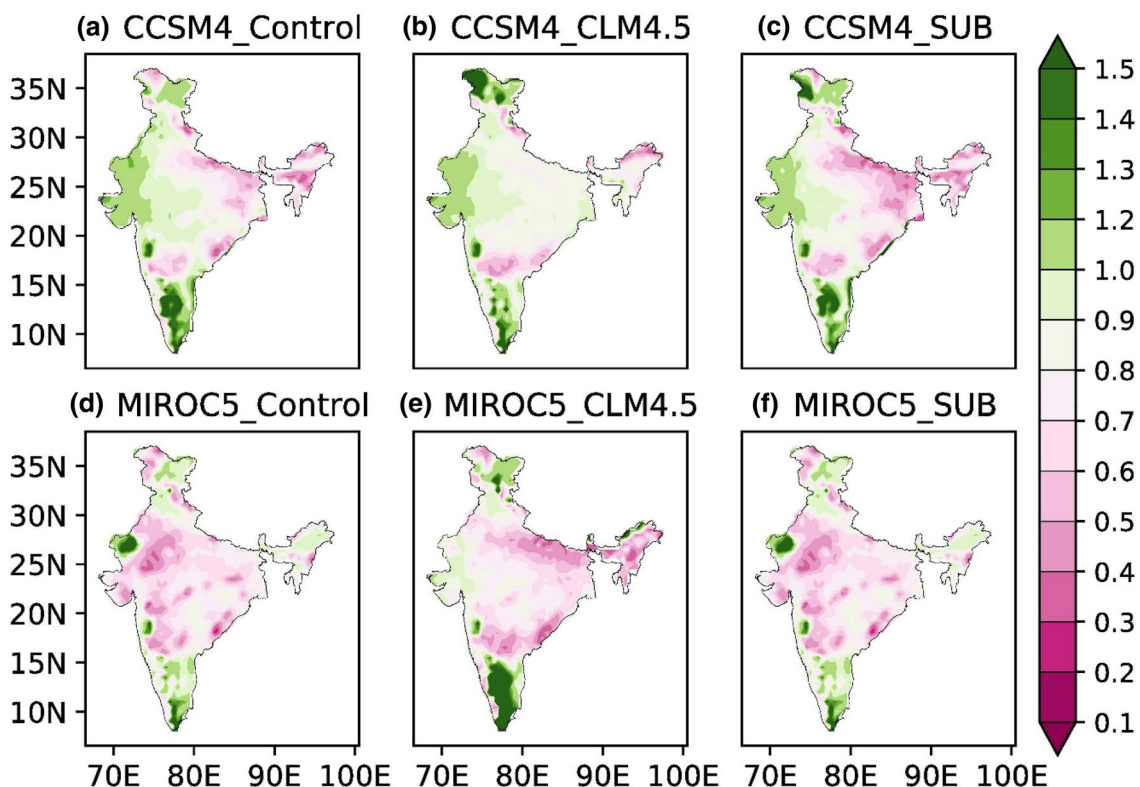

Fig. 9 Normalized root mean squared error (NRMSE) for JJAS precipitation over the Indian region for the period 1975–2005 computed against IMD observation

IOA across the region. Following the spatial patterns of IOA, it has been found that the CCSM4 set of experiments has a lesser agreement in precipitation representation over the central and peninsular India. This is also true for the MIROC5_SUB experiment, as this also has a lesser agreement index (0.1–0.2) over the central and northeast India. Overall, MIROC5_CLM4.5 (Fig. 10e) experiment shows greater spatial coverage in terms of higher IOA values. It is interesting to note that most of the experiments are capable of representing precipitation with higher degrees of agreement over the northwestern and peninsular Indian region, which generally experiences an overall less rainfall during the monsoon season. The degree of agreement in simulating the precipitation in the case of MIROC5_CLM4.5 is of the order of 0.2–0.5, which is the highest from the suite of six experiments.

3.5.3 Taylor metrics

For a comprehensive assessment of the model performance, a multi-metric diagram proposed by Taylor (2001) has been used and presented in Fig. 11. These metrics include the standard deviation, RMSE and correlation co-efficient between different variables of the modeled and observed atmosphere. Using these metrics, the best performing model is selected based on the highest correlation, along with the lowest standard deviation and RMSE values. The variables used for comparing Taylor's metrics are namely: Precipitation, T_{mean}, zonal and meridional winds at 850 hPa and Total cloud fraction. Overall, the MIROC5_CLM4.5 experiment displayed the highest correlation with the observation for all the variables; however, the magnitude of RMSE and the standard deviation is comparable to other experiments in many cases. In the case of all the experiments, T_{mean} has been simulated with the highest degree of correlation as all the experiments have correlation values > 0.95. The lowest correlation among all the variables has been observed in the case of precipitation, with the maximum correlation values of 0.5. It is also found that weaker circulation in all the experiments may have origin in poorly simulated V-wind at 850 hPa. Apart from the MIROC5_CLM4.5 experiment, the remaining experiments have inferior performance in simulating the total cloud fraction. Thus they possibly lead to larger dry biases in the precipitation simulation. Moreover, there are great inter-model differences among models with different land-surface parameterization as well as the GCM forcing. As discussed previously in Sect. 3.2, CCSM4_CLM4.5 is another experiment, which can capture the cross-equatorial flow as well as the moisture transport more realistically as compared to the ERA-Interim dataset. Such corroboration
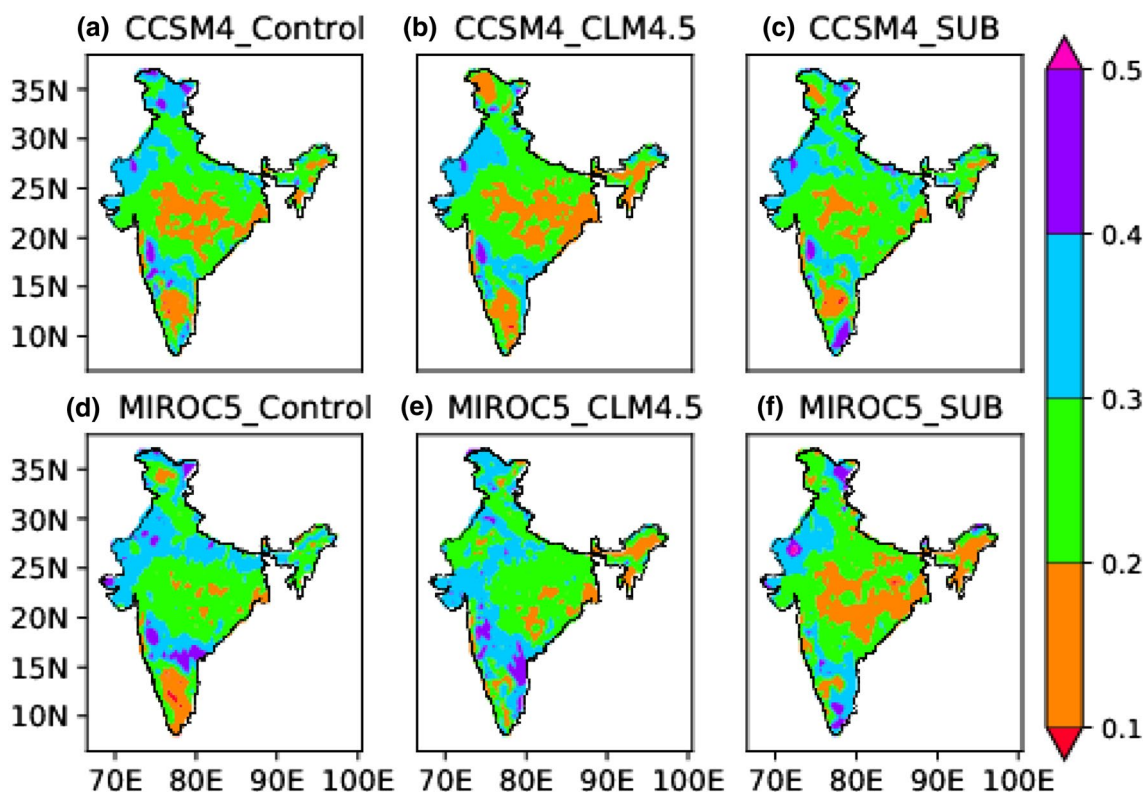

Fig. 10 Willmott's Index of Agreement (Willmott 1982) for precipitation against IMD observation for the period 1975–2005 over the Indian landmass
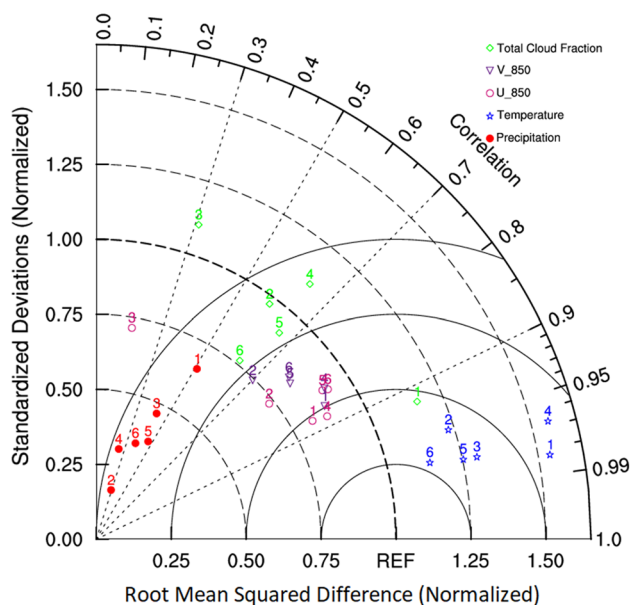
Fig. 11 Taylor's diagram and the associated metrics for different variables (symbols in different colors) and experiments for the period 1970–2005. The numbers represent: 1, MIROC5_CLM4.5; 2, MIROC5_Control; 3, MIROC5_SUB; 4, CCSM4_CLM4.5; 5, CCSM4_Control and 6, CCSM4_SUB experiments respectively

becomes more reinforced with the fact that both the experiments with CLM4.5 have similar values of the correlation coefficient, standard deviation and RMSE for both U and V-wind at 850 hPa. However, they have considerable differences in the simulation of total cloud cover and precipitation over the study area, which may be related to incorrect patterns and magnitudes of moisture convergence in the CCSM4_CLM4.5 experiment.

3.6 Physical mechanisms

In order to understand the reasons behind the inherent biases in the model simulation and the role of land-surface coupling thereon, a process-based investigation in terms of various dynamical, surface and thermodynamical quantities have been carried out. A detailed account on such deliberations are being presented in the following paragraphs.

3.6.1 Surface energy balance

To assess the differences in the surface energy balance in different experiments, JJAS mean sensible heat flux (SHF) and latent heat flux (LHF) climatology are analyzed (Figs. 12, 13). The negative values of SHF signify that the sensible heat is moving towards the surface, while for LHF, it indicates that soil water is evaporating from the surface. The spatial pattern of SHF for Control and SUB-BATS experiments driven by the same

GCM are found to simulate identical patterns of mean SHF largely. The only slight difference is there over the higher reaches of northwestern Himalaya where negative values have been simulated. Similar to the previous, MIROC5_Control and MIROC5_SUB experiments have similar spatial patterns of SHF and LHF. This signifies that in the simulation surface fluxes, Control and SUB-BATS schemes behave similarly and have very nominal differences in subgrid dis-aggregation. Contrasting to Control and SUB-BATS model integrations, CLM4.5 experiments tend to simulate higher magnitudes of SHF (Fig. 12b, e) and lower magnitudes of LHF (Fig. 13b, e). This helps in improving the simulation of T_{mean} in these sets of simulations with comparatively less bias, as discussed in Figs. 2 and 3. The greater sensible heating in the case of CCSM4_CLM4.5 manifests as stronger warm bias, while the lesser sensible heating in the case of MIROC5_Control and MIROC5_SUB experiments end up inducing a moderate cold bias in these experiments. Moreover, greater LHF values over the major part of Indian landmass have been simulated in the case of Control and SUB-BATS experiments compared to CLM4.5 experiments. This feature is more prominent in the experiments forced with CCSM4 GCM. This not only has implications in terms of the surface energy balance in the case of these experiments but may also have influenced the formulation of an appropriate land–sea gradient of temperature and pressure. This may have originated in the formation of higher-pressure regions over land, which offsets the convective activities and thus affects the large-scale south-westerlies at lower levels. Higher (lower) values of LHF (SHF) induces a weak monsoon circulation with less heating over land in case of Control and SUB-BATS experiments and the moisture convergence over land is also subsequently weak in such scenarios. The flux partitioning over the Indian landmass in different experiments may also be explained in terms of the availability of surface soil moisture (top layer, 0.1 m). The spatial distribution of soil moisture (Fig. 14) is in consistent agreement with the spatial patterns of SHF and LHF. For instance, the Control and SUB-BATS experiments have been found to have a comparatively saturated top layer especially over the central, peninsular and northeastern region. The saturated top layer possibly facilitates greater absorption of heat in the surface soil moisture and thus higher (lower) values of LHF (SHF) are apparently seen in the case of these experiments. Lower sensible heating near the surface constrains the warming of the adjacent air and thus, the vertical movement of an overlying air parcel is affected. Such a mechanism is reversed in the case of CLM4.5 experiments where lower values of surface soil moisture are simulated, which induces sensible heating and thus the favorable conditions for the
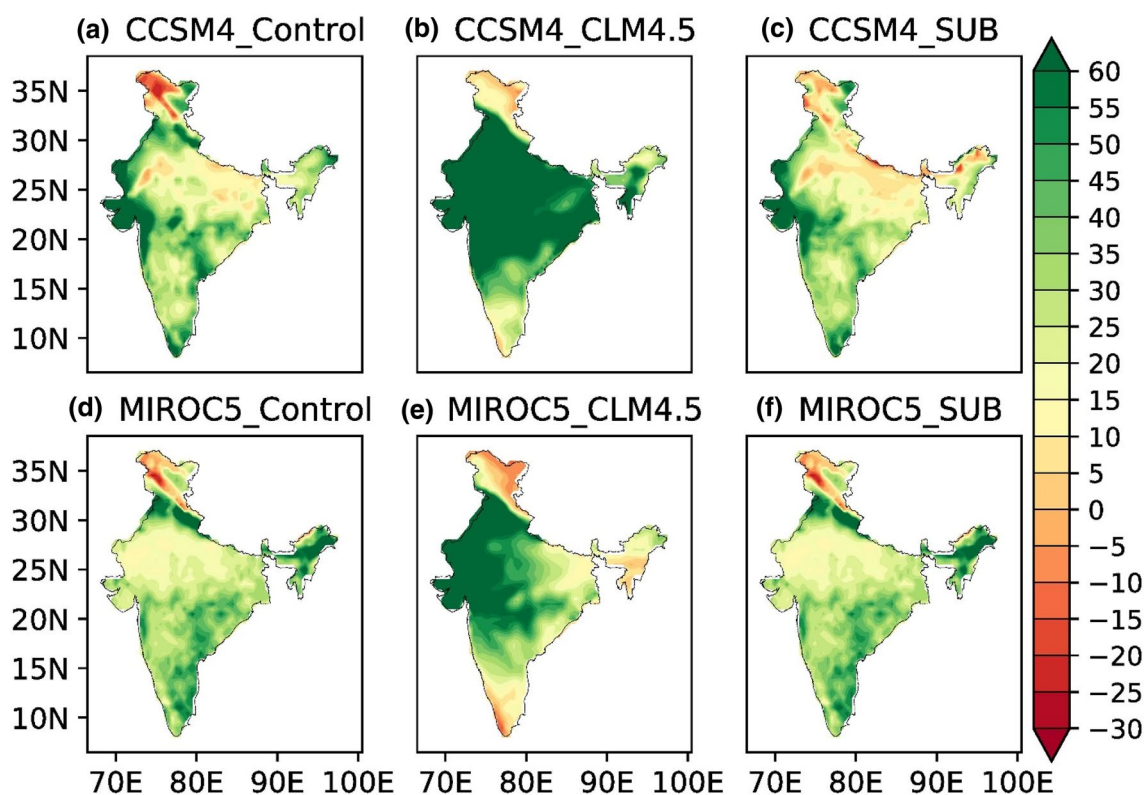
Fig. 12 Sensible heal flux (W m^{-2}) during JJAS season over the Indian landmass for the period 1975–2005 from different experiments

triggering of convection at the surface. The spatial patterns of the fluxes also explain the patterns of temperature bias in the discussed experiments closely. The experiments with greater sensible heating produce lesser biases in T_{mean} simulation.

3.6.2 Tropospheric temperature gradient

The tropospheric temperature is defined as the average of the 600–200 hPa temperature. The gradient of the tropospheric temperature between north and south has been widely used as an objective criterion for studying the onset and withdrawal of the ISM in many studies. The TTG is responsible for driving the meridional circulation over the ISM region (Webster et al. 1998). For assessing the intensity of the model-simulated land–sea gradient and the monsoonal circulation, TTG has been presented from ERA-Interim reanalysis and different model experiments in Fig. 15. It is found that most of the experiments seem to have a weaker gradient in terms of their magnitude as well as the temporal evolution during the ISM season. The estimated values from the ERA-Interim dataset suggest a systematic evolution of TTG with magnitude ≥ 3 K during the peak ISM months i.e. July–August. In comparison to this, all the experiments underestimate the value and typically simulate late-onset

and early withdrawal of monsoon than the reanalysis. The overall important characteristics of TTG, such as the onset, withdrawal, time evolution during the season as well as magnitude, are well represented in the case of the experiments forced with MIROC5. As indicated in Fig. 15, the experiments forced with MIROC5 correlates quite well with the ERA-Interim reanalysis. Furthermore, the MIROC5_CLM4.5 experiment resembles the temporal evolution of TTG with the highest correlation value (0.98), thus indicating a better land–sea contrast as compared to other experiments. The climatology of the 600–200 hPa averaged tropospheric temperature suggests that a warmer atmospheric column has been simulated in case of the experiments forced with CCSM4 (Fig. S4 and S5). Such a warmer atmosphere tends to weaken and offset the large-scale TTG and thus possibly has weaker dynamics of monsoon associated with it during the season.

Exploring further, the patterns of simulated vertical motions in the case of individual experiments, latitude-pressure diagram for vertical velocity (ω, Pa/s) has been presented in Fig. 16. The vertical motion in the atmosphere is an essential factor for the transfer of mass and energy in the atmosphere as it is related to the process of cloud formation and affects the atmospheric stability. It is known that ISM is a convectively coupled phenomenon, and the large-scale
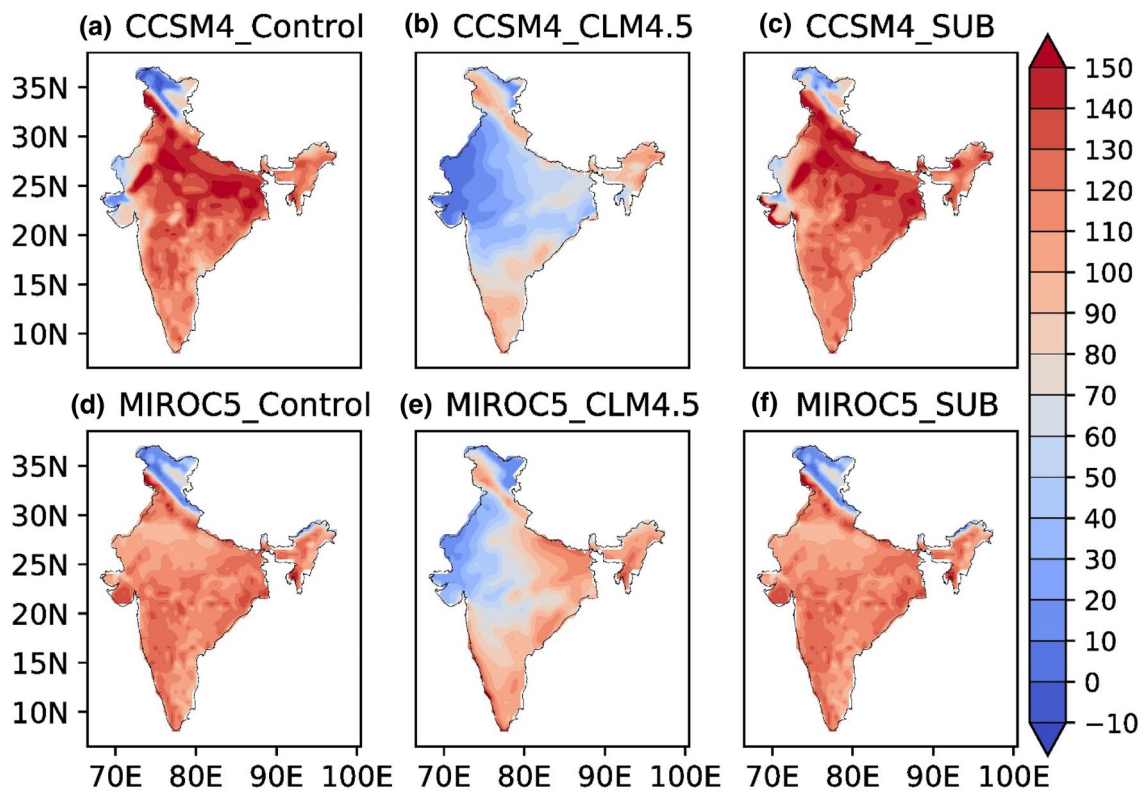
Fig. 13 Same as Fig. 12, but for latent heat flux (W m^{-2})

circulation has considerable impacts on the simulation of monsoon convection and thus the precipitation in a modeling framework. It was also shown that the precipitation biases over central India were likely to be related to the regional Hadley circulation during monsoon (Slingo and Annamalai 2000). The negative values of ω signify the rising upward motion while the positive values describe the subsiding air masses. All the experiments underestimate the magnitude of omega over the region when compared to ERA-Interim estimates (figure not shown). A strong rising motion in the case of Control and SUB-BATS experiments forced with the MIROC5 model has been seen over the equatorial region. This rising air mass extends deep in the atmosphere in such experiments, which may indicate the strong convection over equatorial regions. Such a feature is absent in the case of CCSM4 set of simulations except for CCSM4_CLM4.5 experiment which has comparatively weaker rising motion extending below mid-troposphere. This may also be one of the reasons for weaker moisture convergence and subsequent precipitation biases in these model simulations. It is said that the regional circulations e.g. Hadley cell, are the response of differential heating. This means a rising branch often generates near a heat source while descending branch subsides near a heat sink. A rising branch near the equatorial region, indicating an active convection belt along with another

rising branch near 26–29° N latitude regions adjacent to the Tibetan plateau are prominently simulated in case of MIROC5_CLM4.5 experiment (Fig. 16e). Such a simulated feature completes the general notion of a possible overturning Hadley cell over the region during monsoon season.

On the other hand, the rising branch over the Tibetan plateau (26–29° N) in the case of MIROC5_Control and MIROC5_SUB experiments are comparatively weaker and thus, the rising limb over the equatorial northern Indian Ocean dominates in this case. This indicates the role of possible higher heating over the tropical Indian Ocean as compared to the Tibetan plateau. The stronger convection cells over the tropical region may also explain the excessive precipitation over the ocean in these two simulations. Overall, the MIROC5_CLM4.5 experiment represents the general features of monsoonal circulation better than other experiments, thereby outperforming other models in simulating the precipitation features over Indian landmass and adjacent regions. The possible reason for better regional vertical motion as well as the Hadley circulation can be described in terms of the interplay of surface flux partitioning and its subsequent feedback to the atmospheric column at regional scales. For instance, unrealistic sensible heating in the case of CCSM4 experiments results in a warmer atmospheric column. This possibly results in a warmer
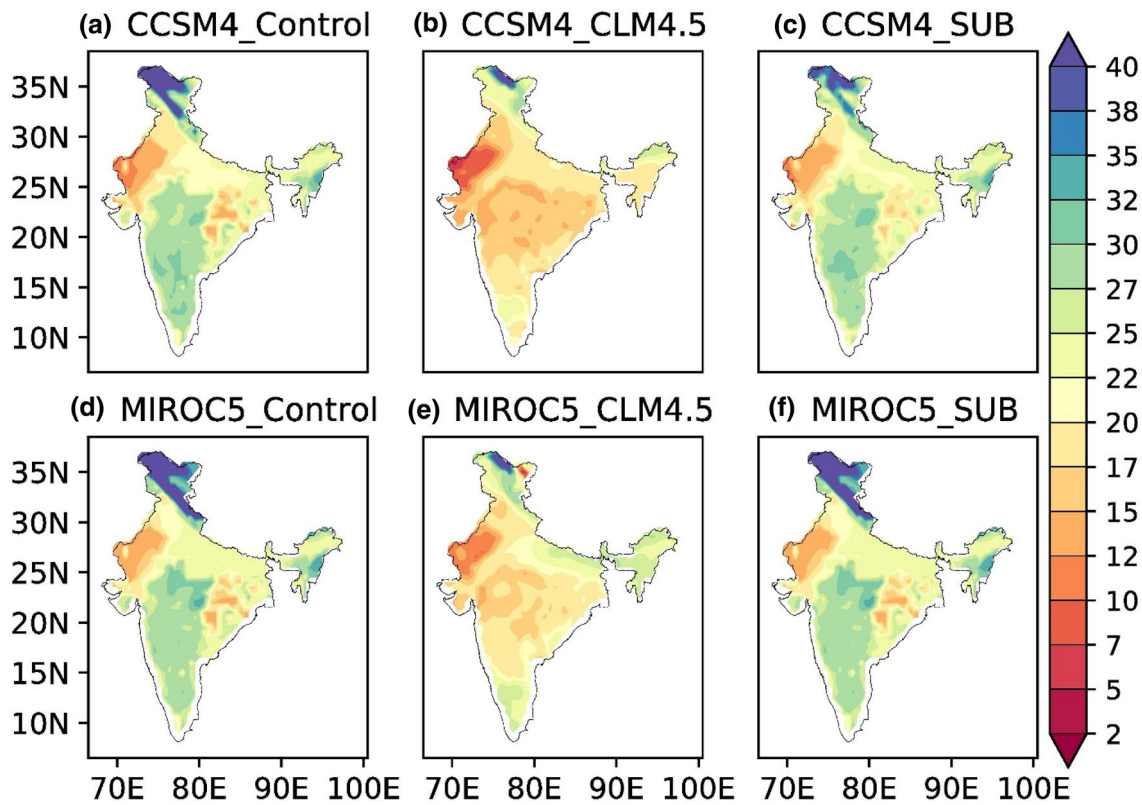
Fig. 14 Mean surface soil moisture content (kg/m^2) for JJAS season from different experiments during 1975–2005. The top layer in Control and SUB-BATS are available at 0.10 m while for CLM4.5 experiments at 0.118865065 m depth

Fig. 15 Tropospheric temperature (600–200 hPa) gradient between the northern (15–35° N, 40–100° E) and southern box (15° S–5° N, 40–100° E) for JJAS season from ERA-Interim reanalysis (black) and different experiments. The values in color corresponds to the correlation of different experiments with the reanalysis
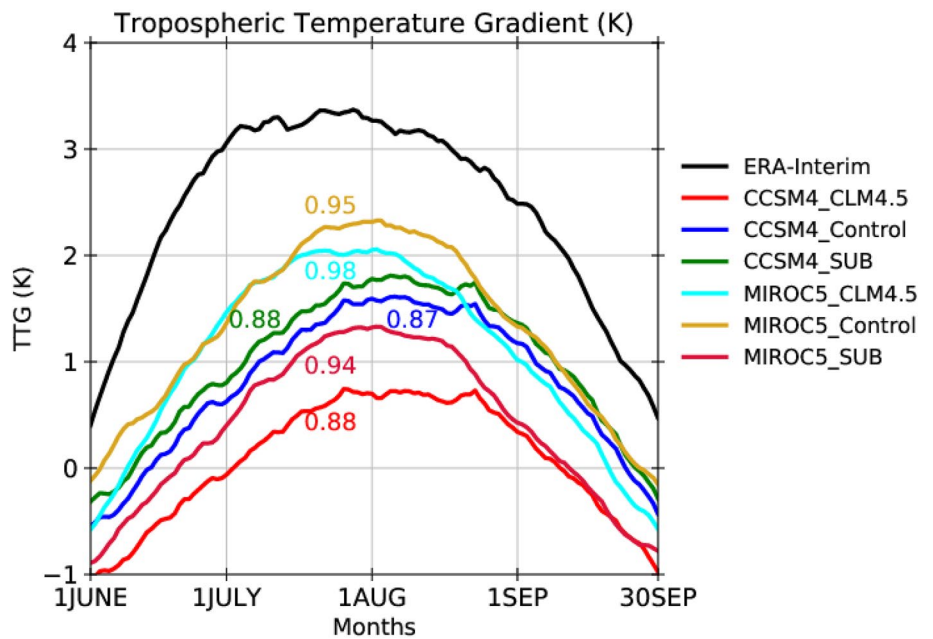
atmosphere and thus a weaker N–S gradient of tropospheric temperature. The better simulation of Hadley circulation in the case of MIROC5_CLM4.5 experiments may be due to

the synergistic effect of better-resolved surface processes i.e. flux partitioning, soil moisture and surface hydrology along with better-simulated TTG.
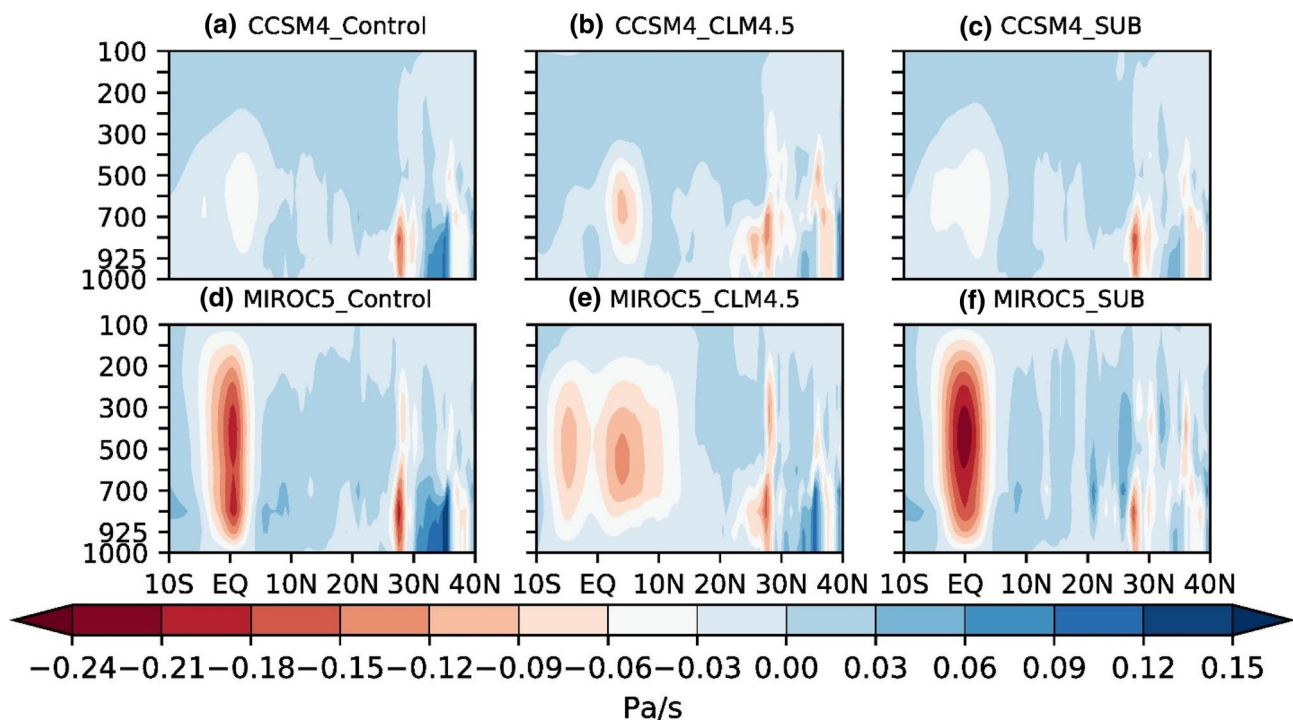
Fig. 16 Latitude-pressure profile of ω (Pa/s) averaged over 70–90° E longitude for the JJAS season during 1975–2005 from different experiments. By convention, the negative (positive) values represent rising (sinking) motion

4 Summary and conclusions

Simulation of ISM using RCMs has been an important area of research in recent times. This has included the assessment of ISM in representing the mean ISM features including the large scale flow, regional features of monsoonal precipitation, variability at different time scales and also the possible changes in the future climate. Previous studies have shown that the reliability of regionally downscaled information depends upon the physical parameterization as well as the initial and lateral boundary conditions. Moreover, it has been pointed out that the selection of appropriate land surface parameterization is also crucial for the ISM simulation. This becomes even important in the case of the studies aiming for future projections at regional levels. In lieu of this, an objective approach has been adopted in this work for studying the efficacy of appropriate GCM forcing and land surface parameterization schemes. Based on the available studies, two different GCMs capable of representing the large-scale features and variability of ISM have been chosen for downscaling experiments. This results in a set of six-different experiments corresponding to two GCMs and three-land surface parameterization schemes for the present climate (1975–2005). The analysis of simulated experiments for JJAS season in terms of various statistical metrics suggests that models have inherent biases in the representation of different features of ISM. These biases are dependent on

the initial forcing, i.e. GCM as well as the choice of land surface parameterization. These biases are also different for different regions over the study area. For the simulation of T_{mean}, it is found that the CLM4.5 experiments simulate warmer climatology and bias irrespective of the GCM forcing. While a dissimilar response of Control and SUB-BATS experiments has been noticed as the experiments forced with CCSM4 and MIROC5 display warm and cold biases over Indian landmass respectively. Such experiments also lead to weaker low-level circulation and subsequent weaker moisture transport over the land regions. A consistent dry bias in all model simulations has been found, following the weaker large-scale dynamics. Despite consistent dry biases in all the experiments, the MIROC5_CLM4.5 experiment outperforms others in simulating the spatial distribution, mean annual cycle, and the probability distribution of daily mean JJAS precipitation.

Further statistical analysis in terms of NRMSE, Willmott's Index of agreement and Taylor's diagram suggests a better performance in the case of the MIROC5_CLM4.5 experiment. The reason for such better performance has been investigated and it has been found that a more realistic representation of the land surface processes especially the partitioning of sensible and latent heat fluxes, prevails in this case. This leads to better representation of the land–sea temperature gradient further manifesting into an appropriate low-level circulation and moisture transport.

Moreover, most of the experiments seem to have constrained vertical motion, which possibly results in inhibition of convection over land areas. Such features are well-simulated in the case of the CLM4.5 experiment forced with the MIROC5 model. A better-resolved regional Hadley cell, in this case, can be attributed to the surface flux partitioning and its feedback to the atmospheric column. This possibly results in more realistic TTG, thus allowing better dynamical response in monsoon simulation in this experiment. This indicates a promising performance of the CLM4.5 coupled land surface model in the simulation of ISM over the Indian region. Evidently, the MIROC5 GCM has more utility in driving the RegCM model for studying the present climate. The overall better performance of MIROC5_CLM4.5 arises due to the interactions of a better representation of surface processes, appropriate GCM boundary forcing and the choice of cumulus parameterization. Additionally, further tuning of parameters in the convection scheme or comparison of the same MIROC5_CLM4.5 experiment with convection scheme other than MIT-Emanuel may also provide a better comparative sense of performance especially in reference of ISM subject to further verification.

References

Alapaty K, Raman S, Madala RV, Mohanty UC (1994) Monsoon rainfall simulations with the Kuo and Betts-Miller schemes. Meteorol Atmos Phys 53(1–2):33–49

Ali S, Dan L, Fu C, Yang Y (2015) Performance of convective parameterization schemes in Asia using RegCM: simulations in three typical regions for the period 1998–2002. Adv Atmos Sci 32(5):715–730

Babar ZA, Zhi XF, Fei G (2015) Precipitation assessment of Indian summer monsoon based on CMIP5 climate simulations. Arab J Geosci 8(7):4379–4392

Bhaskaran B, Jones RG, Murphy JM, Noguer M (1996) Simulations of the Indian summer monsoon using a nested regional climate model: domain size experiments. Clim Dyn 12(9):573–587

Bhaskaran B, Murphy JM, Jones RG (1998) Intraseasonal oscillation in the Indian summer monsoon simulated by global and nested regional climate models. Mon Weather Rev 126(12):3124–3134

Bhate J, Unnikrishnan CK, Rajeevan M (2012) Regional climate model simulations of the 2009 Indian summer monsoon. Indian J Radio Space Phys 41:488–500

Bhatla R, Ghosh S, Mandal B, Mall RK, Sharma K (2016) Simulation of Indian summer monsoon onset with different parameterization convection schemes of RegCM-4.3. Atmos Res 176:10–18

Bretherton CS, Peters ME, Back LE (2004) Relationships between water vapor path and precipitation over the tropical oceans. J Clim 17(7):1517–1528

Chakraborty A, Nanjundiah RS, Srinivasan J (2002) Role of Asian and African orography in Indian summer monsoon. Geophys Res Lett 29(20):50–51

Choudhary A, Dimri AP, Maharana P (2018) Assessment of COR-DEX-SA experiments in representing precipitation climatology of summer monsoon over India. Theoret Appl Climatol 134(1–2):283–307

Choudhary A, Dimri AP, Paeth H (2019) Added value of CORDEX-SA experiments in simulating summer monsoon precipitation over India. Int J Climatol 39(4):2156–2172

Das L, Dutta M, Mezghani A, Benestad RE (2018) Use of observed temperature statistics in ranking CMIP5 model performance over the Western Himalayan Region of India. Int J Climatol 38(2):554–570

Dash SK, Singh GP, Shekhar MS, Vernekar AD (2005) Response of the Indian summer monsoon circulation and rainfall to seasonal snow depth anomaly over Eurasia. Clim Dyn 24(1):1–10

Dash SK, Shekhar MS, Singh GP (2006) Simulation of Indian summer monsoon circulation and rainfall using RegCM3. Theor Appl Climatol 86(1–4):161–172

Dee DP, Uppala SM, Simmons AJ, Berrisford P, Poli P, Kobayashi S, Bechtold P (2011) The ERA-Interim reanalysis: configuration and performance of the data assimilation system. Q J R Meteorol Soc 137(656):553–597

Dhar ON, Nandargi S (2003) Hydrometeorological aspects of floods in India. Nat Hazards 28(1):1–33

Dickinson E, Henderson-Sellers A, Kennedy J (1993) Biosphere–atmosphere transfer scheme (BATS) version 1e as coupled to the NCAR community climate model

Dimri AP, Niyogi D (2013) Regional climate model application at subgrid scale on Indian winter monsoon over the western Himalayas. Int J Climatol 33(9):2185–2205

Dobler A, Ahrens B (2010) Analysis of the Indian summer monsoon system in the regional climate model COSMO-CLM. J Geophys Res Atmos. https://doi.org/10.1029/2009JD013497

Fasullo J, Webster PJ (2003) A hydrological definition of Indian monsoon onset and withdrawal. J Clim 16(19):3200–3211

Fennessy MJ, Kinter JL III, Kirtman B, Marx L, Nigam S, Schneider E, Zhou J (1994) The simulated Indian monsoon: a GCM sensitivity study. J Clim 7(1):33–43

Gadgil S, Vinayachandran PN, Francis PA, Gadgil S (2004) Extremes of the Indian summer monsoon rainfall. Geophys Res Lett, ENSO and equatorial Indian Ocean oscillation. https://doi.org/10.1029/2004GL019733

Gao XJ, Shi Y, Giorgi F (2016) Comparison of convective parameterizations in RegCM4 experiments over China with CLM as the land surface model. Atmos Ocean Sci Lett 9(4):246–254

Giorgi F, Francisco R, Pal J (2003) Effects of a subgrid-scale topography and land use scheme on the simulation of surface climate and hydrology. Part I: effects of temperature and water vapor disaggregation. J Hydrometeorol 4(2):317–333

Giorgi F, Coppola E, Solmon F, Mariotti L, Sylla MB, Bi X, Turuncoglu UU (2012) RegCM4: model description and preliminary tests over multiple CORDEX domains. Clim Res 52:7–29

Goswami BN (2005) South Asian monsoon. In: Intraseasonal variability in the atmosphere–ocean climate system. Springer, Berlin, pp 19–61

Goswami BN, Mohan RA (2001) Intraseasonal oscillations and interannual variability of the Indian summer monsoon. J Clim 14(6):1180–1198

Goswami BN, Madhusoodanan MS, Neema CP, Sengupta D (2006a) A physical mechanism for North Atlantic SST influence on

the Indian summer monsoon. Geophys Res Lett. https://doi.org/10.1029/2005GL024803

Goswami BN, Venugopal V, Sengupta D, Madhusoodanan MS, Xavier PK (2006b) Increasing trend of extreme rain events over India in a warming environment. Science 314(5804):1442–1445

Guhathakurta P, Rajeevan M (2008) Trends in the rainfall pattern over India. Int J Climatol 28(11):1453–1469

Hahn DG, Shukla J (1976) An apparent relationship between Eurasian snow cover and Indian monsoon rainfall. J Atmos Sci 33(12):2461–2462

Harris IC, Jones PD (2017) CRU TS4.00: Climatic Research Unit (CRU) Time-Series (TS) version 4.00 of high resolution gridded data of month-by-month variation in climate (Jan. 1901–Dec. 2015). Centre for Environmental Data Analysis, 25

Holtslag AAM, De Bruijn EIF, Pan HL (1990) A high resolution air mass transformation model for short-range weather forecasting. Mon Weather Rev 118(8):1561–1575

Iqbal W, Syed FS, Sajjad H, Nikulin G, Kjellström E, Hannachi A (2017) Mean climate and representation of jet streams in the CORDEX South Asia simulations by the regional climate model RCA4. Theor Appl Climatol 129(1–2):1–19

Jacob D, Podzun R (1997) Sensitivity studies with the regional climate model REMO. Meteorol Atmos Phys 63(1–2):119–129

Jena P, Azad S, Rajeevan M (2016) CMIP5 projected changes in the annual cycle of Indian monsoon rainfall. Climate 4(1):14

Ji Y, Vernekar AD (1997) Simulation of the Asian summer monsoons of 1987 and 1988 with a regional model nested in a global GCM. J Clim 10(8):1965–1979

Kang S, Im ES, Ahn JB (2014) The impact of two land-surface schemes on the characteristics of summer precipitation over East Asia from the RegCM4 simulations. Int J Climatol 34(15):3986–3997

Kiehl T, Hack J, Bonan B, Boville A, Briegleb P, Williamson L, Rasch J (1996) Description of the NCAR community climate model (CCM3)

Kripalani RH, Kulkarni A, Sabade SS, Khandekar ML (2003) Indian monsoon variability in a global warming scenario. Nat Hazards 29(2):189–206

Kumar D, Dimri AP (2019) Sensitivity of convective and land surface parameterization in the simulation of contrasting monsoons over CORDEX-South Asia domain using RegCM-4.4.5.5. Theor Appl Climatol. https://doi.org/10.1007/s00704-019-02976-9

Kumar KR, Pant GB, Parthasarathy B, Sontakke NA (1992) Spatial and subseasonal patterns of the long-term trends of Indian summer monsoon rainfall. Int J Climatol 12(3):257–268

Kumar KK, Rajagopalan B, Hoerling M, Bates G, Cane M (2006) Unraveling the mystery of Indian monsoon failure during El Niño. Science 314(5796):115–119

Lim YJ, Hong J, Lee TY (2012) Spin-up behavior of soil moisture content over East Asia in a land surface model. Meteorol Atmos Phys 118(3–4):151–161

Lucas-Picher P, Christensen JH, Saeed F, Kumar P, Asharaf S, Ahrens B, Hagemann S (2011) Can regional climate models represent the Indian monsoon? J Hydrometeorol 12(5):849–868

Maharana P, Dimri AP (2016) Study of intraseasonal variability of Indian summer monsoon using a regional climate model. Clim Dyn 46(3–4):1043–1064

Maity S, Mandal M, Nayak S, Bhatla R (2017a) Performance of cumulus parameterization schemes in the simulation of Indian Summer Monsoon using RegCM4. Atmósfera 30(4):287–309

Maity S, Satyanarayana ANV, Mandal M, Nayak S (2017b) Performance evaluation of land surface models and cumulus convection schemes in the simulation of Indian summer monsoon using a regional climate model. Atmos Res 197:21–41

Martínez-Castro D, da Rocha RP, Bezanilla-Morlot A, Alvarez-Escudero L, Reyes-Fernández JP, Silva-Vidal Y, Arritt RW (2006) Sensitivity studies of the RegCM3 simulation of summer precipitation, temperature and local wind field in the Caribbean Region. Theor Appl Climatol 86(1–4):5–22

Maurya RKS, Sinha P, Mohanty MR, Mohanty UC (2017) Coupling of community land model with RegCM4 for Indian summer monsoon simulation. Pure Appl Geophys 174(11):4251–4270

Maurya RKS, Sinha P, Mohanty MR, Mohanty UC (2018) RegCM4 model sensitivity to horizontal resolution and domain size in simulating the Indian summer monsoon. Atmos Res 210:15–33

Meehl GA (1994) Influence of the land surface in the Asian summer monsoon: external conditions versus internal feedbacks. J Clim 7(7):1033–1049

Meher JK, Das L, Akhter J, Benestad RE, Mezghani A (2017) Performance of CMIP3 and CMIP5 GCMs to simulate observed rainfall characteristics over the Western Himalayan region. J Clim 30(19):7777–7799

Menon A, Levermann A, Schewe J, Lehmann J, Frieler K (2013) Consistent increase in Indian monsoon rainfall and its variability across CMIP-5 models. Earth Syst Dyn 4:287–300

Mishra V, Kumar D, Ganguly AR, Sanjay J, Mujumdar M, Krishnan R, Shah RD (2014) Reliability of regional and global climate models to simulate precipitation extremes over India. J Geophys Res Atmos 119(15):9301–9323

Mohan RA, Goswami BN (2003) Potential predictability of the Asian summer monsoon on monthly and seasonal time scales. Meteorol Atmos Phys 84(1–2):83–100

Mooley DA, Parthasarathy B (1983) Indian summer monsoon and El Nino. Pure Appl Geophys 121:339–352. https://doi.org/10.1007/BF02590143

Mukhopadhyay P, Taraphdar S, Goswami BN, Krishnakumar K (2010) Indian summer monsoon precipitation climatology in a high-resolution regional climate model: impacts of convective parameterization on systematic biases. Weather Forecast 25(2):369–387

Nayak S, Mandal M, Maity S (2017) Customization of regional climate model (RegCM4) over Indian region. Theor Appl Climatol 127(1–2):153–168

Pal JS, Small EE, Eltahir EA (2000) Simulation of regional-scale water and energy budgets: representation of subgrid cloud and precipitation processes within RegCM. J Geophys Res Atmos 105(D24):29579–29594

Pant GB, Parthasarathy SB (1981) Some aspects of an association between the southern oscillation and Indian summer monsoon. Arch Meteorol Geophys Bioclimatol Ser B 29(3):245–252

Prasanna V (2016) Assessment of South Asian summer monsoon simulation in CMIP5-coupled climate models during the historical period (1850–2005). Pure Appl Geophys 173(4):1379–1402

Rai P, Joshi M, Dimri AP, Turner AG (2018) The role of potential vorticity anomalies in the Somali Jet on Indian Summer Monsoon Intraseasonal Variability. Clim Dyn 50(11–12):4149–4169

Rajeevan M, Bhate J (2009) A high resolution daily gridded rainfall dataset (1971–2005) for mesoscale meteorological studies. Curr Sci 96:558–562

Rajeevan M, Bhate J, Kale JD, Lal B (2006) High resolution daily gridded rainfall data for the Indian region: analysis of break and active. Curr Sci 91(3):296–306

Rajeevan M, Rohini P, Kumar KN, Srinivasan J, Unnikrishnan CK (2013) A study of vertical cloud structure of the Indian summer monsoon using CloudSat data. Clim Dyn 40(3–4):637–650

Raju PVS, Bhatla R, Almazroui M, Assiri M (2015) Performance of convection schemes on the simulation of summer monsoon features over the South Asia CORDEX domain using RegCM-4.3. Int J Climatol 35(15):4695–4706

Rao DVB, Ashok K, Yamagata T (2004) A numerical simulation study of the Indian summer monsoon of 1994 using NCAR MM5. J Meteorol Soc Jpn Ser II 82(6):1755–1775

Ratnam JV, Cox EA (2006) Simulation of monsoon depressions using MM5: sensitivity to cumulus parameterization schemes. Meteorol Atmos Phys 93(1–2):53–78

Ratnam JV, Kumar KK (2005) Sensitivity of the simulated monsoons of 1987 and 1988 to convective parameterization schemes in MM5. J Clim 18(14):2724–2743

Ratnam JV, Giorgi F, Kaginalkar A, Cozzini S (2009) Simulation of the Indian monsoon using the RegCM3–ROMS regional coupled model. Clim Dyn 33(1):119–139

Roxy MK, Ritika K, Terray P, Murtugudde R, Ashok K, Goswami BN (2015) Drying of Indian subcontinent by rapid Indian Ocean warming and a weakening land–sea thermal gradient. Nat Commun 6:7423

Saeed F, Hagemann S, Jacob D (2009) Impact of irrigation on the South Asian summer monsoon. Geophys Res Lett. https://doi.org/10.1029/2009GL040625

Saha SK, Halder S, Kumar KK, Goswami BN (2011) Pre-onset land surface processes and 'internal' interannual variabilities of the Indian summer monsoon. Clim Dyn 36(11–12):2077–2089

Sarthi PP, Ghosh S, Kumar P (2015) Possible future projection of Indian Summer Monsoon Rainfall (ISMR) with the evaluation of model performance in Coupled Model Inter-comparison Project Phase 5 (CMIP5). Glob Planet Change 129:92–106

Sarthi PP, Kumar P, Ghosh S (2016) Possible future rainfall over Gangetic Plains (GP), India, in multi-model simulations of CMIP3 and CMIP5. Theor Appl Climatol 124(3–4):691–701

Sharmila S, Joseph S, Sahai AK, Abhilash S, Chattopadhyay R (2015) Future projection of Indian summer monsoon variability under climate change scenario: an assessment from CMIP5 climate models. Glob Planet Change 124:62–78

Singh GP, Oh JH (2007) Impact of Indian Ocean sea-surface temperature anomaly on Indian summer monsoon precipitation using a regional climate model. Int J Climatol 27(11):1455–1465

Singh AP, Singh RP, Raju PVS, Bhatla R (2011) The impact of three different cumulus parameterization schemes on the Indian summer monsoon circulation. Int J Ocean Clim Syst 2(1):27–43

Singh S, Ghosh S, Sahana AS, Vittal H, Karmakar S (2017) Do dynamic regional models add value to the global model projections of Indian monsoon? Clim Dyn 48(3–4):1375–1397

Sinha P, Mohanty UC, Kar SC, Kumari S (2014) Role of the Himalayan orography in simulation of the Indian summer monsoon using RegCM3. Pure Appl Geophys 171(7):1385–1407

Sinha P, Maurya RKS, Mohanty MR, Mohanty UC (2019) Inter-comparison and evaluation of mixed-convection schemes in RegCM4 for Indian summer monsoon simulation. Atmos Res 215:239–252

Slingo JM, Annamalai H (2000) 1997: the El Niño of the century and the response of the Indian summer monsoon. Mon Weather Rev 128(6):1778–1797

Sooraj KP, Terray P, Mujumdar M (2015) Global warming and the weakening of the Asian summer monsoon circulation: assessments from the CMIP5 models. Clim Dyn 45(1–2):233–252

Srinivas CV, Hariprasad D, Bhaskar Rao DV, Anjaneyulu Y, Baskaran R, Venkatraman B (2013) Simulation of the Indian summer monsoon regional climate using advanced research WRF model. Int J Climatol 33(5):1195–1210

Taylor KE (2001) Summarizing multiple aspects of model performance in a single diagram. J Geophys Res Atmos 106(D7):7183–7192

Tiwari PR, Kar SC, Mohanty UC, Dey S, Sinha P, Raju PVS, Shekhar MS (2015) The role of land surface schemes in the regional climate model (RegCM) for seasonal scale simulations over Western Himalaya. Atmósfera 28(2):129–142

Tiwari PR, Kar SC, Mohanty UC, Dey S, Sinha P, Shekhar MS (2017) Sensitivity of the Himalayan orography representation in simulation of winter precipitation using Regional Climate Model (RegCM) nested in a GCM. Clim Dyn 49(11–12):4157–4170

Umakanth U, Kesarkar AP, Raju A, Rao SVB (2016) Representation of monsoon intraseasonal oscillations in regional climate model: sensitivity to convective physics. Clim Dyn 47(3–4):895–917

Van Zomeren J, Van Delden A (2007) Vertically integrated moisture flux convergence as a predictor of thunderstorms. Atmos Res 83(2–4):435–445

Wang Y, Sen OL, Wang B (2003) A highly resolved regional climate model (IPRC-RegCM) and its simulation of the 1998 severe precipitation event over China. Part I: model description and verification of simulation. J Clim 16(11):1721–1738

Webster PJ, Magana VO, Palmer TN, Shukla J, Tomas RA, Yanai MU, Yasunari T (1998) Monsoons: processes, predictability, and the prospects for prediction. J Geophys Res Oceans 103(C7):14451–14510

Willmott CJ (1982) Some comments on the evaluation of model performance. Bull Am Meteorol Soc 63(11):1309–1313

Xavier PK, Marzin C, Goswami BN (2007) An objective definition of the Indian summer monsoon season and a new perspective on the ENSO–monsoon relationship. Q J R Meteorol Soc 133(624):749–764